



Universidade de Brasília

Instituto de Ciências Exatas
Departamento de Ciência da Computação

**Accelerating Sensitivity Analysis in Microscopy
Image Segmentation Workflows with Multi-level
Computation and Data Reuse**

Willian de Oliveira Barreiros Júnior

Dissertação apresentada como requisito parcial para
conclusão do Mestrado em Informática

Orientador
Prof. Dr. George Luiz Medeiros Teodoro

Brasília
2018

Ficha Catalográfica de Teses e Dissertações

Está página existe apenas para indicar onde a ficha catalográfica gerada para dissertações de mestrado e teses de doutorado defendidas na UnB. A Biblioteca Central é responsável pela ficha, mais informações nos sítios:

<http://www.bce.unb.br>

<http://www.bce.unb.br/elaboracao-de-fichas-catalograficas-de-teses-e-dissertacoes>

Esta página não deve ser inclusa na versão final do texto.



Universidade de Brasília

Instituto de Ciências Exatas
Departamento de Ciência da Computação

Accelerating Sensitivity Analysis in Microscopy Image Segmentation Workflows with Multi-level Computation and Data Reuse

Willian de Oliveira Barreiros Júnior

Dissertação apresentada como requisito parcial para
conclusão do Mestrado em Informática

Prof. Dr. George Luiz Medeiros Teodoro (Orientador)
CIC/UnB

Prof.a Dr.a Alba Cristina Magalhães Alves de Melo Dr. Eduardo Adílo Pelinson Alchieri
CIC/UnB CIC/UnB

Prof. Dr. Bruno Macchiavello
Coordenador do Programa de Pós-graduação em Informática

Brasília, 10 de fevereiro de 2018

Dedicatória

Ao meu pai...

Agradecimentos

Nos *agradecimentos*, o autor se dirige a pessoas ou instituições que contribuíram para elaboração do trabalho apresentado. Por exemplo: *Agradeço aos gigantes cujos ombros me permitiram enxergar mais longe. E a Google e Wikipédia.*

Resumo

Com a crescente disponibilidade de equipamentos de imagens microscópicas médicas existe uma demanda para execução eficiente de aplicações de processamento de imagens *whole slide tissue*. Pelo processo de análise de sensibilidade é possível melhorar a qualidade dos resultados de tais, e subsequentemente, a qualidade da análise realizada a partir deles. Devido ao alto custo computacional e à natureza recorrente das tarefas executadas por métodos de análise de sensibilidade (i.e., reexecução de tarefas), emergem oportunidades para reuso computacional. Pela realização de reuso computacional otimiza-se o tempo de execução das aplicações de análise de sensibilidade. Este trabalho tem como objetivo encontrar novas maneiras de aproveitar as oportunidades de reuso computacional em múltiplos níveis de abstração das tarefas computacionais. Isto é feito pela apresentação de algoritmos de reuso de tarefas grão-grosso e de novos algoritmos de reuso de tarefas grão-fino, implementados no *Region Templates Framework*.

Palavras-chave: Reuso Computacional, Analise de Sensibilidade, *Region Templates Framework*

Abstract

With the increasingly availability of digital microscopy imagery equipment there is a demand for efficient execution of whole slide tissue image applications. Through the process of sensitivity analysis we can improve the output quality of such applications, and thus, improve the desired analysis quality. Due to the high computational cost of such analyses and the recurrent nature of executed tasks from sensitivity analysis methods (i.e., reexecution of tasks), the opportunity for computation reuse arises. By performing computation reuse we can optimize the run time of sensitivity analysis applications. This work focus then on finding new ways to take advantage of computation reuse opportunities on multiple task abstraction levels. This is done by presenting the coarse-grain merging strategy and the new fine-grain merging algorithms, implemented on top of the Region Templates Framework.

Keywords: Computation Reuse, Sensitivity Analysis, Region Templates Framework

Sumário

1	Introduction	1
1.1	The Problem	3
1.2	Goals	3
1.3	Work Structure/Organization	4
2	Background	5
2.1	Microscopy Image Analysis	5
2.2	Sensitivity Analysis	6
2.3	Region Templates Framework (RTF)	8
2.4	Computation Reuse	10
3	Multi-Level Computation Reuse: Completed Activities	13
3.1	Graphical Interface and Code Generator	15
3.2	Stage-Level Merging	17
3.3	Task-Level Merging	18
3.3.1	Naïve Algorithm	19
3.3.2	Smart Cut Algorithm (SCA)	19
3.3.3	Reuse Tree Merging Algorithm (RTMA)	21
3.3.4	Task-Balanced Reuse Tree Merging Algorithm (TRMA)	25
4	Experimental Results	33
4.1	Experimental Environment	33
4.2	Impact of Multi-level Computation Reuse and SA methods	33
4.2.1	Impact of Multi-level Computation Reuse for MOAT	34
4.2.2	Impact of Multi-level Computation Reuse for VBD	35
4.3	Impact of Bucket Size and Its Effect on Parallelism	36
4.4	Worst-Case Scalability Analysis	37
5	Schedule	39

Listas de Figuras

2.1	An example microscopy image analysis workflow. Image extracted from [1].	5
2.2	An example of tissue image segmentation.	6
2.3	The main components of the Region Templates Framework, highlighting the steps of a coarse-grain stage instance execution. Image extracted from [26].	8
2.4	The execution of a stage instance from the perspective of a node, showing the fine-grain tasks scheduling. Image extracted from [26].	9
3.1	The parameter study framework. An SA method selects parameters of the analysis workflow, which is executed on a parallel machine. The workflow results are compared to a set of reference results to compute differences in the output. This process is repeated a set number of times (sample size) with varying input parameters' values.	13
3.2	A comparison of a workflow generated with and without computation reuse. Image extracted from [27].	14
3.3	An example stage descriptor XML file.	15
3.4	The example workflow described with the Taverna Workbench.	16
3.5	An example on which SCA executes on 5 instances of a workflow application of 6 tasks, with $MaxBucketSize = 2$.	20
3.6	An example where node x is inserted on the existing reuse tree. Figure 3.6a defines the tasks of which each stage is composed by and presents the parameters' values for each stage instance.	22
3.7	An example of Reuse Tree based merging with $MaxBucketSize = 3$. The merged stages of each step are shown below the tree on the bucket list.	23
3.8	Simple example of <i>Full-Merge</i> on which $MaxBuckets$ is 3 and the exact division of stages is reached.	26
3.9	Another example of <i>Full-Merge</i> and <i>Fold-Merge</i> on which $MaxBuckets$ is 3 and the exact division of stages cannot be reached by <i>Full-Merge</i> .	27
3.10	An example of the <i>Balance</i> step on which there are 3 buckets to be balanced.	28

3.11 A general worst-case reuse-tree representation on which we have all n stages divided into b buckets. On this case we have $b - 1$ buckets with exactly one stage, and thus cost k . Hence, the last bucket has $n - b + 1$ stages. For this last bucket we assume the single and uniform reuse of the first r task, having no reuse for the remaining $k - r$ tasks. This is the worst-case for balancement applications.	30
3.12 An example reuse-tree that can be used to illustrate possible prunable nodes. E.g., the use of nodes 4, 5, 6, or 10, 11 as an improvement attempt results in the same outcome (cost 3), making them interchangeable, as with nodes 7, 8 or 9 (cost 4), or nodes 12-22 (cost 3).	31
4.1 Impact of the computation reuse for different strategies as the sample size of the MOAT analysis is varied.	34
4.2 Impact of the computation reuse strategies for the VBD SA method. . . .	35
4.3 Impact of varying <i>MaxBucketSize</i>	36
4.4 Comparison of the Coarse-grain-only approach with the RTMA and TRMA. .	37

Lista de Tabelas

2.1 Definition of parameters and range values: parameter space contains about 21 trillion points.	7
5.1 Schedule of activities for 2017.	39

Capítulo 1

Introduction

We define algorithm sensitivity analysis (SA) as the process of quantifying, comparing, and correlating output from multiple analyses of a dataset computed with variations of an analysis workflow using different input parameters [22]. This process is executed in many phases of scientific research and can be used to quantify the impact of changes in input parameters to differences in the workflow output.

The main motivation of this work is the use of image analysis workflows for whole slide tissue images analysis [13], which extracts salient information from tissue images in the form of segmented objects (e.g., cells) as well as their shape and texture features. Imaging features computed by such workflows contain rich information that can be used to develop morphological models of the specimens under study to gain new insights into disease mechanisms and assess disease progression.

A concern with automated biomedical image analysis is that the output quality of analysis workflows is highly sensitive to changes in the input parameters. As such, adaptation of SA methods and methodologies employed in other fields [18], [29], [3], [10], can help better evaluate an image analysis workflows for both developers and users. In short, the benefits of SA include: (i) better assessment and understanding of the correlation between input parameters and analysis output; (ii) the ability to reduce the uncertainty/-variation of the analysis output by identifying the causes of variation; and (iii) workflow simplification by fixing parameters values' or removing parts of the code that have limited or negligible effect on the output.

Although the benefits of using SA are many, its use in practice is onerous given the data and computation challenges associated with it. For instance, a single study using a classic method such as MOAT (Morris One-At-Time) [18] may require hundreds of runs (sample size) of the image analysis workflow. The execution of a single Whole Slide Tissue Image (WSI) will extract about 400,000 nuclei on average and can take hours on a single computing node. A study at scale will consider hundreds of WSIs and compute millions of

nuclei per run, which need to be compared to a reference dataset of objects to assess and quantify differences as input parameters are varied by the SA method. A single analysis at this scale using a moderate sample size with 240 parameter sets and 100 WSI would take at least three years if executed sequentially [26]. Given how time consuming such analysis is, there is a demand to develop mechanisms to make it feasible, such as parallel execution of tasks and computation reuse.

Computation reuse in hierarchical workflows is the process of reusing routines results instead of re-executing them. Computation reuse opportunities arise when distinct computation tasks have the same input parameters, thus being unnecessary the re-execution of such task. Seizing reuse opportunities is done by a merging process, in which two or more task are merged together, after which the repeated portions of the merged tasks are set to execute only once.

Computation reuse on this work will be accomplished with the use of fine-grain tasks merging algorithms, to be integrated on top of the Region Templates Framework (RTF) platform. This platform is responsible for the distributed execution of hierarchical workflows in large scale computation environments, also abstracting dependency resolution and file management. It is important to highlight that the RTF already implements a similar form of computation reuse in the form of coarse-grain tasks reuse, and that the new fine-grain merging algorithm must improve the performance of SA applications alongside the existing coarse-grain merging algorithm.

Other works perform computation reuse as a mean to reduce overall computational cost in different ways and for distinct goals [19, 23, 21, 28, 17, 24, 11, 12]. Although the principle of computation reuse is rather abstract, its implementation on this work is distinct from all found existing methods and, as a consequence, it is impossible the direct comparison between methods.

This work proposes two ways of accomplishing computation reuse in SA, (i) coarse-grain tasks reuse and (ii) fine-grain tasks reuse. The main differences between them is the granularity of the tasks to be reused and the underlying restrictions of the system used to execute these tasks. The reuse of coarse-grain tasks can offer a greater speedup when reuse happens, but there are less reuse opportunities. With fine-grain tasks these reuse opportunities are more frequent, however, more sophisticated strategies need to be employed in order to deal with dependency resolution and to avoid performance degradation due to reduced parallelism.

1.1 The Problem

Because of high computing demands, sensitivity analysis applied to microscopy image analysis is unfeasible for routinely use when applied to whole slide tissue images.

1.2 Goals

This work focuses on improving the performance of SA studies in microscopy image analysis through the application of computation reuse.

The specific goals of this work are presented below. Each of the goals we have already targeted have a reference to the section in which we describe the work completed

1. Modify the RTF to use a graphic interface for the deployment of workflows [Section 3.1];
2. Upgrade the RTF to enable the use of fine-grain tasks [Section 3.1];
3. Develop and analyze algorithms for multi-level reuse:
 - (a) Propose and implement a coarse-grain merging algorithm [Section 3.2];
 - (b) Propose and implement a fine-grain naïve merging algorithm [Section 3.3.1];
 - (c) Propose and implement a fine-grain smart cut merging algorithm [Section 3.3.2];
 - (d) Propose and implement a fine-grain reuse tree merging algorithm [Section 3.3.3];
4. Optimize existing fine-grain merging algorithms
 - (a) Improve the reuse factor of the reuse tree merging algorithm by performing a 2-level pruning operation [Section ??] **Eu ainda não escrevi essa parte já que os resultados experimentais não foram consistentes: tem caso que melhora a performance, tem caso que não faz nada. Coloca no texto essa otimização ou apaga?;**
 - (b) Evaluate and reduce unbalance on the reuse tree merging algorithm [Section 3.3.4];
 - (c) Evaluate and deal with memory constraint problems [Section ??] **Essa é aquela estratégia de execução com o valor correto de MaxBuckets para não estourar a memória. Coloca no texto?;**

5. Demonstrate the performance gains of the proposed algorithms with a real microscopy image analysis application, using different SA strategies (e.g MOAT and VBD) at different scales.

1.3 Work Structure/Organization

The next section describes the motivating application, the theory behind computation reuse and the Region Templates Framework (RTF), which was used to deploy the application on a parallel machine and is also the tool in which the merging algorithms were incorporated. Section III describes what has been done so far, including some fine-grain merging algorithms and preliminary results. In Section IV, tasks that we plan to perform until the end of this work are described. Finally, Section V presents a schedule for the remaining of tasks.

Capítulo 2

Background

This chapter describes the motivating application along with the Region Templates Framework, in which this work is developed, and some basic concepts of sensitivity analysis and computation reuse.

2.1 Microscopy Image Analysis

It is now possible for biomedical researchers to capture highly detailed images from whole slide tissue samples in a few minutes with high-end microscopy scanners, which are becoming evermore available. This capability of collecting thousands of images on a daily basis extends the possibilities for generating detailed databases of several diseases. Through the investigation of tissue morphology of whole slide tissue images (WSI) there is the possibility of better understanding disease subtypes and feature distributions, enabling the creation of novel methods for classification of disease state. With the increasing number of research groups working and developing richer methods for carrying out quantitative microscopy image analyses [8, 20, 15, 6, 7, 4, 5, 16] and also the increasingly availability of digital microscopy imagery equipment, there is a high demand for systems or frameworks oriented towards the efficient execution of microscopy image analysis workflows.

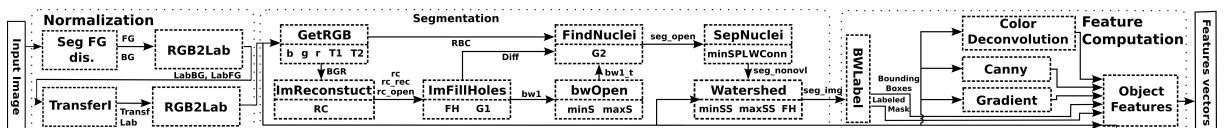


Figura 2.1: An example microscopy image analysis workflow. Image extracted from [1].

The microscopy image analysis workflow used on this work is presented in Figure 2.1. This workflow consists of normalization, segmentation, feature computation and final classification, being the first three analysis stages the most computationally expensive

phases. The first stage is responsible for normalizing the staining and/or illumination conditions of the image. The segmentation is the process of identifying the nucleus of each cell of the analyzed image (Figure 2.2). Through feature computation a set of shape and texture features is generated of each segmented nucleus. Finally, the final classification will typically involve using data mining algorithms on aggregated information, by which some insights on the underlying biological mechanism that enables the distinction of subtypes of diseases are gained.

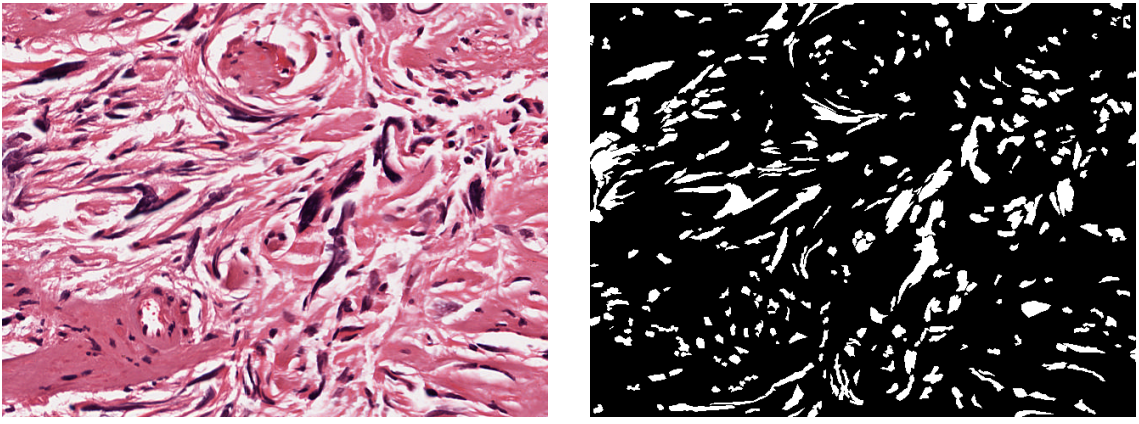


Figura 2.2: An example of tissue image segmentation.

The quality of the workflow analysis is, however, dependent of the parameters values, described in Table 2.1. Therefore, in order to improve the effectiveness of the analysis the impact of these parameters on the output of the used workflow (Figure 2.1) should be analyzed. This impact analysis is known as sensitivity analysis and will be detailed on the next section.

2.2 Sensitivity Analysis

We define Sensitivity Analysis (SA) as the process of quantifying, comparing and correlating the input parameters of a workflow with the intent of quantifying the impact of each input to the final output of the workflow [22]. This process is applied on several phases of scientific research including, but not limited to model validation, parameter studies and optimization, and error estimation.

Usually, the computational cost for performing SA on a workflow is directly proportional to the number of parameters it has. Furthermore, a large number of parameters makes the analysis of these workflows more difficult both from the logical and compu-

tational cost standpoints. One way to simplify the analysis is through the removal of parameters whose effect on the output is negligible.

This work focus on extending the already existing system, the Region Templates Framework (RTF) [26, 27], which performs sensitivity analysis in two phases. On the first phase the 15 input parameters (Table 2.1) are screened with a light SA method used to remove the so called non-influential parameters from the next phase. Afterwards, a second SA method is executed on the remaining parameters, on which both first-order and high-order effects of these on the application output are quantified.

The light SA method, Morris One-At-A-Time (MOAT) [18], performs a series of runs of the application changing each parameter individually, while fixing the remaining parameters, using a discretized parameter search space. Each of the k analyzed parameters value ranges are uniformly partitioned in p levels, thus resulting in a p^k grid of parameter sets to be evaluated. Each evaluation x_i of the application creates a parameter elementary effect (EE), calculated as $EE_i = \frac{y(x_1, \dots, x_i + \Delta_i, \dots, x_k) - y(x)}{\Delta_i}$, with $y(x)$ being the application output before the parameter perturbation. In order to account for global SA the RTF uses $\Delta_i = \frac{p}{2(p-1)}$ [27]. The MOAT method requires $r(k+1)$ evaluations, with r in the range of 5 to 15 [9].

The second SA method, Variance-Based Decomposition (VBD) is preferably performed after a lighter SA method, as the MOAT method, since it requires $n(k+2)$ evaluations for k parameters and n samples, which can lie in the order of thousands of executions [29]. Thus, a reduced number of parameters is used for feasibility reasons. VBD, unlike MOAT, discriminates the the output uncertainty effects among individual parameters, accounting for first-order and high-order effects.

Parameter	Description	Range Values
B/G/R	Background detection thresholds	[210, 220, ..., 240]
T1/T2	Red blood cell thresholds	[2.5, 3.0, ..., 7.5]
G1/G2	Thresholds to identify candidate nuclei	[5, 10, ..., 80]
MinSize(minS)	Candidate nuclei area threshold	[2, 4, ..., 40]
MaxSize(maxS)	Candidate nuclei area threshold	[900, .., 1500]
MinSizePI (minSPL)	Area threshold before watershed	[5, 10, ..., 80]
MinSizeSeg (maxSS)	Area threshold in final output	[2, 4, ..., 40]
MaxSizeSeg (minSS)	Area threshold in final output	[900, .., 1500]
FillHoles(FH)	propagation neighborhood	[4-conn, 8-conn]
MorphRecon(RC)	propagation neighborhood	[4-conn, 8-conn]
Watershed(WConn)	propagation neighborhood	[4-conn, 8-conn]

Tabela 2.1: Definition of parameters and range values: parameter space contains about 21 trillion points.

The combination of large set of parameters with their rather large values ranges'

(Table 2.1) results in the unfeasible task of performing SA on the workflow of Figure 2.1, which has 21 trillion different parameter sets combinations. For the sake of extenuating this unfeasibility issue for performing SA on the presented workflow we can execute the analysis on high-end distributed computing environments. Also, computation reuse can be employed to reduce the computational cost without the need of application specific optimizations. Both mentioned methods are described in the next sections.

2.3 Region Templates Framework (RTF)

The Region Template Framework (RTF) abstracts the execution of a workflow application on a distributed environment [26]. It supports hierarchical workflows that are composed of coarse-grain stages, which in turn are composed by fine-grain tasks, with all the dependencies being solved by the RTF. Given a homogeneous environment of n nodes with k cores each, any stage instance must be executed on a single node, with its tasks being executed on any or multiple of the k cores of the same node. It is noteworthy that, not only any node can have more than one stage instance executing on it, but also, there may be more than one task from the same stage running in parallel, given that the inter-tasks dependencies are respected.

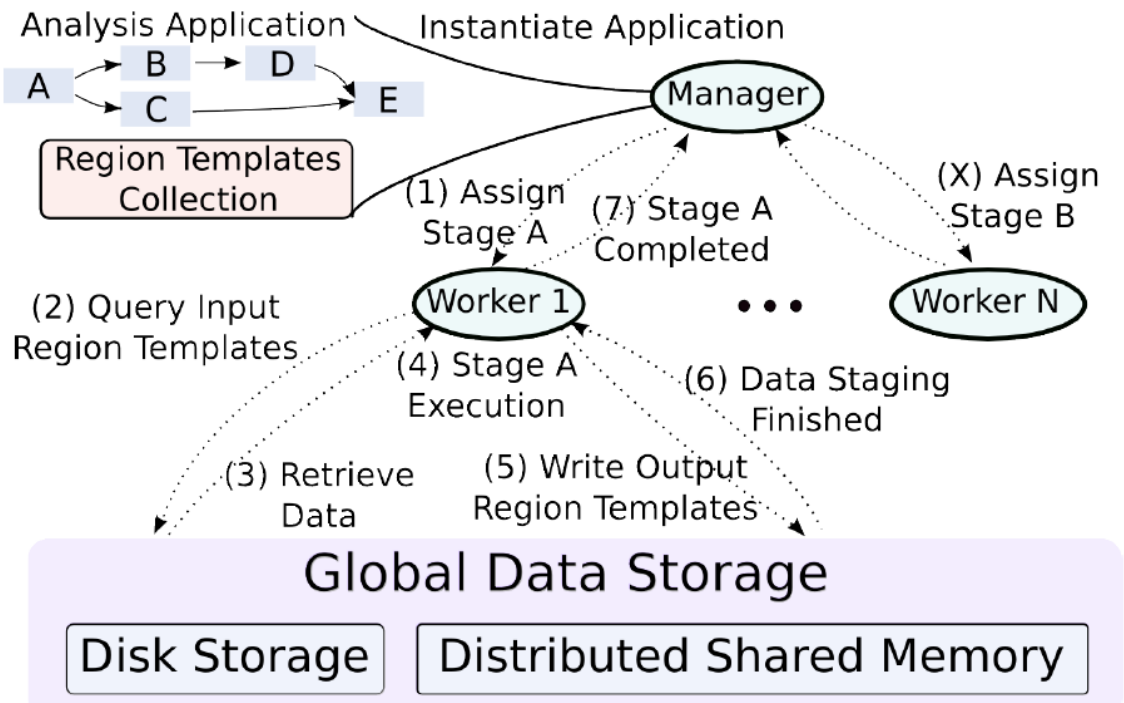


Figura 2.3: The main components of the Region Templates Framework, highlighting the steps of a coarse-grain stage instance execution. Image extracted from [26].

The main components of the RTF are: the data abstraction, the runtime system, and the hierarchical data storage layer [26]. The runtime system consists of core functions for scheduling of application stages, transparent data movement and management via the storage layer, as shown in Figure 2.3 by the communication and distribution of work between the Manager node and the worker nodes. The hierarchical workflow representation allows for different scheduling strategies to be used at each level (stage-level and task-level). Fine-grain scheduling is possible at the second level to exploit variability in performance of application operations in hybrid systems. In Figure 2.4 a stage A is sent to a worker node for execution, which tasks are scheduled locally. Whenever there is a choice of whether executing a given task on a CPU or an accelerator (e.g., GPU) the local scheduler takes into consideration the expected speedup of the task if it is executed on an accelerator, optimizing the overall makespan.

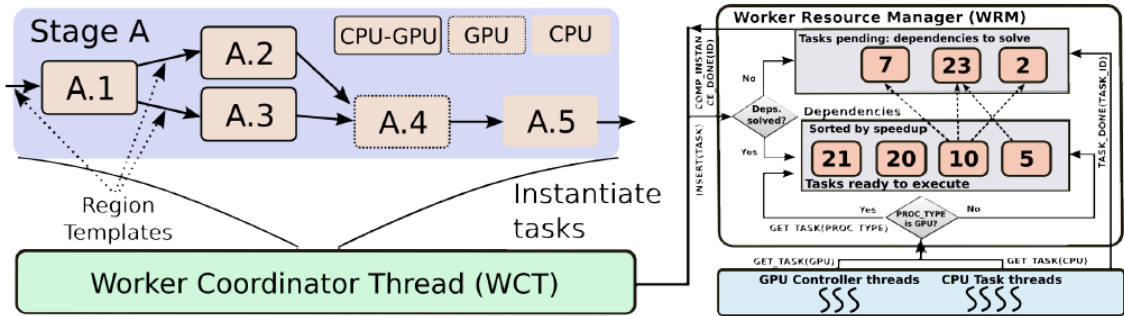


Figura 2.4: The execution of a stage instance from the perspective of a node, showing the fine-grain tasks scheduling. Image extracted from [26].

On the data storage layer the Region Templates (RT) data abstraction is used to represent and interchange data (represented by the collection of objects of an application instance and the stored data of figure 2.3). It consists of storage containers for data structures commonly found in applications that process data in low-dimensional spaces (1D, 2D or 3D spaces) with a temporal component. The data types include: pixels, points, arrays (e.g., images or 3D volumes), segmented and annotated objects and regions, all of which are implemented using the OpenCV [2] library interfaces to simplify their use. A region template data instance represents a container for a region defined by a spatial and temporal bounding box. A data region object is a storage materialization of data types and stores the data elements in the region contained by a region template instance. A region template instance may have multiple data regions.

Access to the data elements in data regions is performed through a lightweight class that encapsulates the data layout, provided by the RT library. Each data region of one or multiple region template instances can be associated with different data storage

implementations, defined by the application designer. With this design the decisions regarding data movement and placement are delegated to the runtime environment, which may use different layers of a system memory to place the data according to the workflow requirements.

The runtime system is implemented through a Manager-Worker execution model that combines a bag-of-tasks execution with workflows. The application Manager creates instances of coarse-grain stages, and exports the dependencies among them. These dependencies are represented as data regions to be consumed/produced by the stages. The assignment of work from the Manager to Worker nodes is performed at the granularity of a stage instance using a demand-driven mechanism, on which each Worker node independently requests stages instances from the Manager whenever it has idle resources. Each node is then responsible for fine-grain task scheduling of the received stage(s) to its local resources.

To develop an application for the RTF the developer needs to provide a library of domain specific data analysis operations (in this case, microscopy image analysis) and implement a simple startup component which generates the desired workflow and starts the execution. The application developer also needs to specify a partitioning strategy for data regions encapsulated by the region templates to support parallel computation of said data regions associated with the respective region templates.

Stages of a workflow consume and produce Region Template (RT) objects, which are handled by the RTF, instead of having to read/write data directly from/to stages or disk. While the interactions between coarse-grain stages are handled by the RTF, the task of writing more complex, fine-grained, stages containing several external, domain specific, fine-grain API calls is significantly harder for application experts. This occurs since the RTF works only with one type of task objects as its runnable interface, not providing an easy way to compose stages using fine-grain tasks. The RTF also supports efficient execution on hybrid systems equipped with CPU and accelerators (e.g, GPUs).

2.4 Computation Reuse

The idea of work reuse has been employed on both the hardware and software fronts with diverse techniques, such as value prediction [19], dynamic instruction reuse [23] and *memoization* [21], with the goal of accelerating applications through the removal of duplicated computational tasks. This concept has been used for runtime optimizations on embedded systems [28], low-level encryption value generation [17] and even stadium designing [24]. All of those approaches can be placed into one of two categories, hardware-

level or software-level reuse. This work focus on the second type since hardware-level reuse requires specific hardware designing, which is not the target of this work.

On software-level reuse two main techniques were noticed, (i) reuse based on pre-execution profiling and (ii) *memoization* of recurrent tasks. The first method [28], although efficient, is rather application dependent and incurs in a pre-execution training step, which could be unfeasible to implement for SA applications given the size of the parameters set domain.

The other common approach is through caching of results of selected executions [21, 11, 12] named *memoization*. This method can virtually be used for any application domain, however, increases in the number of reuse opportunities available are achieved through either more domain-specific selection methods or by increasing the amount of memorized results. Also, in order to reduce the solution searching overhead higher-level operations ought to be used, effectively reducing the potential of reuse. Finally, while the use of *memoization* can easily be brought to multiprocessed environments through the addition of parallel control structures (e.g., locks), when we attempt to bring this approach to a distributed environment there is an additional overhead for coherence enforcement, which can be hard to scale.

Any approach for computation reuse is also defined by the level of abstraction of the analyzed tasks. It is noteworthy that higher-level task reuse (or coarse-grain task reuse) is considerably easier to implement since the granularity of coarse-grain tasks incur in more expensive tasks, and thus resulting in less inner-task communication overhead. Also, working on the coarse-grain granularity level prevents the seizing of partial reuse opportunities.

Finer-grain task reuse can hence explore the missed opportunity of partial reusable coarse-grain tasks, since only the common portion can be reused. This approach is however much more difficult to cope with since the communication overhead between merged tasks is more significant given that fine-grain tasks are computationally less expensive.

Also, for the RTF environment performing stage merging indiscriminately can have a toll on parallelism. This is most prominently seen when analyzing a set of workflows which all of its stages instances have some minor degree of reuse opportunities among themselves. By attempting to maximize the reuse of such stages instances we would at the same time minimize the overall computational cost of the analysis and serialize the execution of the stages to a single node.

On [23] Sodani and Sohi implement a hardware-level *reuse buffer* for some instructions, which if an operation under execution is found, its execution can then be finished and the buffered result be returned. By doing this, Sodani and Sohi claim to have cut down the resources required to execute some instructions while also reducing the length of critical

path of some operations. A similar but distinct hardware-level buffer is proposed on [21] for arithmetic operations.

On software level Wang and Raghunathan propose on [28] the use of computation reuse in order to make embedded applications more energy efficient. This is done by profiling the target application, grouping operations into reuse regions, generating a software-level cache and then doing this process over with new execution data in a feedback loop. This approach draws some similarities with [17], in the sense that low-level software operations are reused through the caching of some results.

Still on software level, but on a higher level of abstraction, [11, 12] proposes the application of computation reuse on high-level complex operations or functions. On [11], complete analysis applications for genetic research can be reused if all input parameters match. This is done with the goal of reproducibility. Finally, [12] analyses reusing fitness calculation results for genetic algorithms applied to protein folding applications. Both approaches use a software-level cache to store reusable results.

When analyzing the above approaches for computation reuse and trying to apply their concepts to our domain of SA, any hardware-level proposal cannot be used. Their use would unnecessarily increase the complexity of the application while making any type of parallelism hard to achieve. Regarding [28] software-level approach, even a simple segmentation analysis application is too expensive for profiling. Moreover, while the flexibility of runtime operation grouping is desirable, the image segmentation analysis workflow used in this work is simple enough to be efficiently analyzed manually. Finally, regardless the level on which computation reuse is applied, caching approaches add an operations layer which needs to be optimized to the specific hardware environment on which it is being executed (e.g., the number of cache levels, cache size and number of blocks, replacement policy). This layer, while being easily implemented for serialized applications can become rather difficult very quickly for distributed applications, on which there needs to be a sense of global coherence among computing nodes. Given these problems, simpler and lighter approaches are required for the proposed computation reuse on SA applications on multiprocessed distributed environments.

Capítulo 3

Multi-Level Computation Reuse: Completed Activities

This work has as its main goal the development of efficient Sensibility Analysis (SA) optimizations through multi-level computation reuse. This chapter further analyzes computation reuse and then describes improvements made to the Region Templates Framework (RTF), which were implemented in order to enable the use of multi-level computation reuse. After that, the new computation reuse approaches are described, along with their advantages and disadvantages.

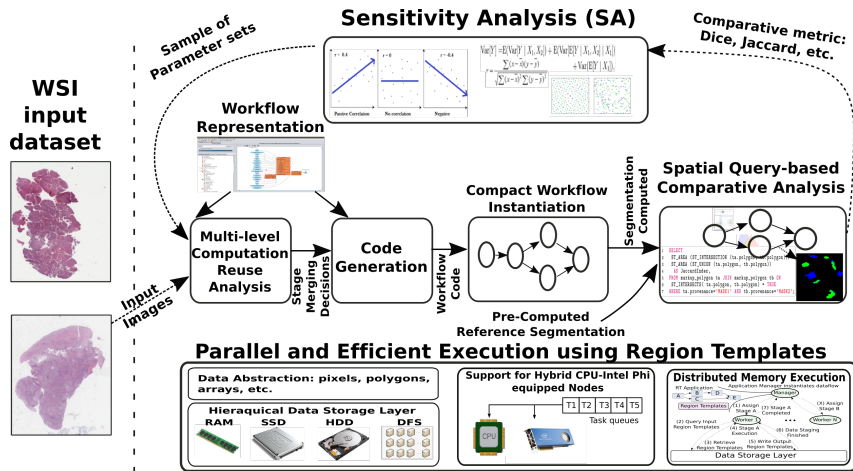


Figura 3.1: The parameter study framework. An SA method selects parameters of the analysis workflow, which is executed on a parallel machine. The workflow results are compared to a set of reference results to compute differences in the output. This process is repeated a set number of times (sample size) with varying input parameters' values.

An scheme of the SA studies and components that were developed and integrated into the RTF are illustrated in Figure 3.1. An SA study in this framework starts with the definition of a given workflow, the parameters to be studied, and the input data.

The workflow is then instantiated and executed efficiently in RT using parameters values selected by the SA method. The output of the workflow is compared using a metric selected by the user to measure the difference between a reference segmentation result and the one computed by the workflow using the parameter set generated by the SA method. One of the metrics to measure difference is Dice, which counts the number of pixels identified as objects (foreground) in both the segmented and computed masks. This process continues until the number of workflow runs does not achieve the sample size required by the SA. This sample size is effectively the number of times that the workflow will be instantiated and executed with different input parameters' values. The sample size is a way to limit the cost of the SA study while maintaining its significance and accuracy.

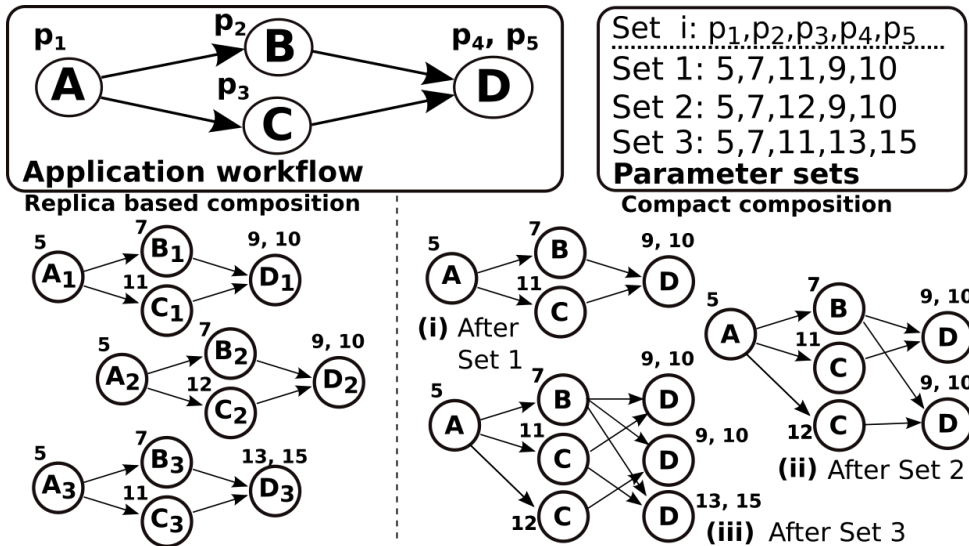


Figura 3.2: A comparison of a workflow generated with and without computation reuse. Image extracted from [27].

Computation reuse is achieved through the removal of repeated computation tasks. Figure 3.2 presents the comparison of a replica-based workflow generation, in which there is no reuse, and a compact composition, generated with maximal reuse. Given that we start generating a compact composition with no tasks on it, the first parameter set (Set 1, (i) in Figure 3.2) is added to the workflow in its entirety. The second parameter set (Set 2, (ii) in Figure 3.2), however, has the reuse opportunities of tasks A and B given they have the same input parameters values and input data. This results in the inclusion of only tasks C and D for parameter set 2 in the compact graph. With the current workflow state ((ii) on Figure 3.2), parameter set 3 presents reuse opportunities for tasks A, B and C, thus only needing to add task D with the parameter value 15 to the workflow. When comparing the workflow replica based composition with the compact composition we can

notice a decrease on the number of executed tasks of approximatively 41%, from 12 tasks to 7 tasks.

There are two computation reuse levels used on this work, (i) stage-level, on which coarse-grain computation tasks are reused, and (ii) task-level, with fine-grain tasks reused. Coarse-grain computation reuse is significantly easier to implement than its fine-grained counterpart. However, the number of parameters that two coarse-grained merging candidates stages need to match is much greater when compared with fine-grain tasks.

3.1 Graphical Interface and Code Generator

In order to implement this work a flexible task-based stage code generator was implemented to ease the process of developing RTF applications. This generator was created, together with a workflow generator graphic interface, with the purpose of making the RTF more accessible to domain-specific experts. Additionally, this code generator will ease the workflow information gathering, necessary for merging stages instances during the process of computation reuse.

```

1  {"name": "Segmentation",
2   "includes": "#include \"opencv2/opencv.hpp\"\n#include \"opencv2/gpu/gpu.hpp\"\n#include\n\"HistologicalEntities.h\"",
3   "dr_args": [
4     {"name": "normalized_rt", "type": "dr", "io": "input"},
5     {"name": "segmented_rt", "type": "dr", "io": "output"}
6   ],
7   "tasks": [
8     {"call": "::nscale::HistologicalEntities::segmentNucleiStg1",
9      "args": [
10        {"name": "normalized_rt", "type": "dr", "io": "input"},
11        {"name": "blue", "type": "uchar"},
12        {"name": "green", "type": "uchar"},
13        {"name": "red", "type": "uchar"},
14        {"name": "T1", "type": "double"},
15        {"name": "T2", "type": "double"}
16      ],
17      "intertask_args": [
18        {"name": "bgr", "type": "mat_vect", "io": "output"},
19        {"name": "rbc", "type": "mat", "io": "output"}
20      ]
21    },
22    {"call": "::nscale::HistologicalEntities::segmentNucleiStg2",
23      "args": [
24        {"name": "reconConnectivity", "type": "int"}
25      ],
26      "intertask_args": [
27        {"name": "bgr", "type": "mat_vect", "io": "input"},
28        {"name": "rbc", "type": "mat", "io": "forward"},
29        {"name": "rc", "type": "mat", "io": "output"},
30        {"name": "rc_recon", "type": "mat", "io": "output"},
31        {"name": "rc_open", "type": "mat", "io": "output"}
32      ],
33    },
34    [...]
35  ],
36  {"call": "::nscale::HistologicalEntities::segmentNucleiStg7",
37    "args": [
38      {"name": "segmented_rt", "type": "dr", "io": "output"},
39      {"name": "minSizeSeg", "type": "int"},
40      {"name": "maxSizeSeg", "type": "int"},
41      {"name": "fillHolesConnectivity", "type": "int"}
42    ],
43    "intertask_args": [
44      {"name": "seg_nooverlap", "type": "mat", "io": "input"}
45    ]
46  }
47 }
48 }
49 }
```

Figura 3.3: An example stage descriptor XML file.

The stage generator has as its input a stage descriptor file, formated as XML, as shown in Figure 3.3. A stage is defined by its name, the external libraries it needs to call in order to execute the application domain transformations in each stage of the workflows, the necessary input arguments for its execution and the tasks it must execute. There are two kinds of inputs, the arguments and the Region Templates (RT). The arguments are constant inputs, which are varied by the given SA method and represent the application input parameter values. The RT is the data structure provided by the RTF for inter-stage and inter-task communication. As seen on the example descriptor file, only the RT inputs are explicitly written, while the remaining arguments can be inferred from the tasks descriptions.

Every stage is comprised of tasks, which are described by (i) the external call to the library of operations implemented by the user and (ii) its arguments. On Figure 3.3 the call for the first task is *segmentNucleiStg1* from the external library *nscale*. The arguments can be one of two types, (i) constant input arguments (args), defined by the SA application or (ii) intertask arguments (intertask_args), which are produced/consumed for/by a fine-grain task.

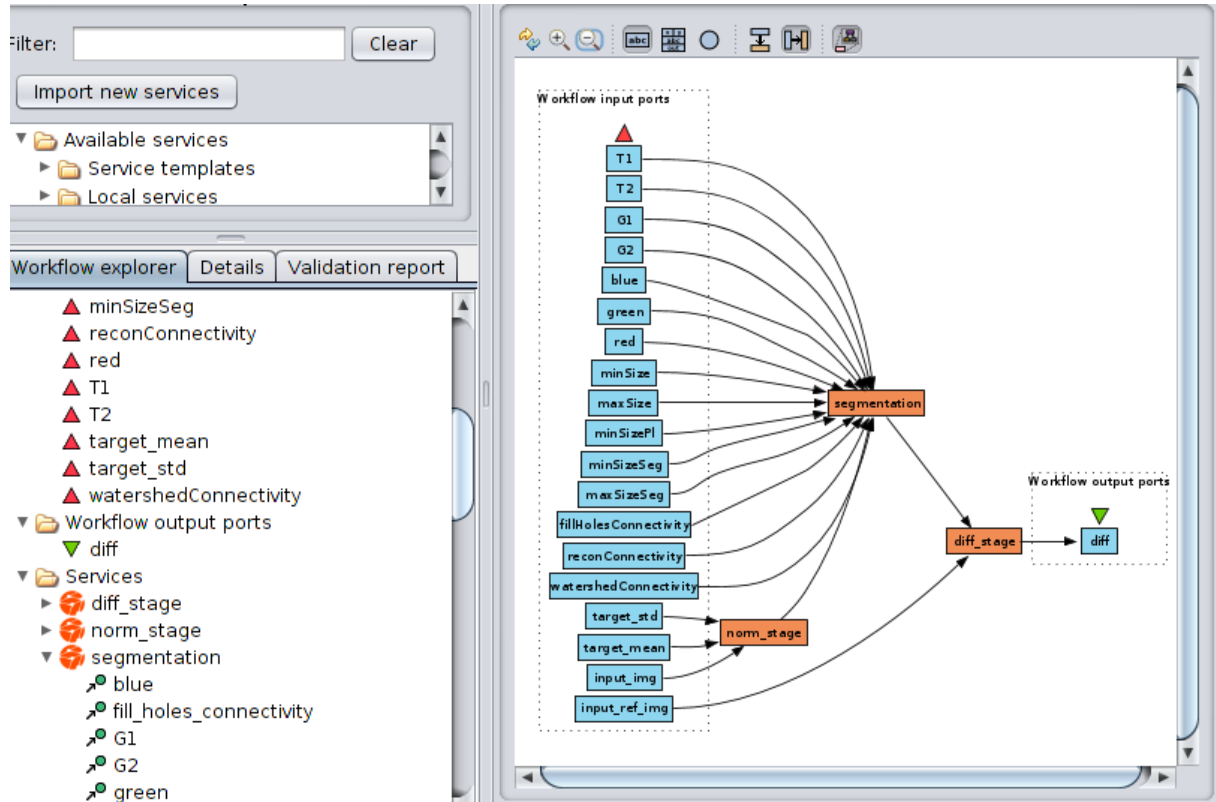


Figura 3.4: The example workflow described with the Taverna Workbench.

With task-based stages generated, the user can make workflows using the newly generated stages. As with tasks, the RTF did not support a non-compiled solution for generating workflows. The solution implemented on this work was to use the Taverna Workbench tool [30] as a graphical interface for producing workflows and implement a parser for the generated Taverna file. An example is displayed on Figure 3.4.

3.2 Stage-Level Merging

The stage level merging needs to identify and remove common stage instances and build a compact representation of the workflow, as presented in Algorithm 1. The algorithm receives the application directed workflow graph (*appGraph*) and parameter sets to be tested as input (*parSets*) and outputs the compact graph (*comGraph*). It iterates over each parameter set (lines 3-5) to instantiate a replica of the application workflow graph with parameters from *set*. It then calls MERGEGRAPH to merge the replica to the compact representation.

The MERGEGRAPH procedure walks simultaneously in an application workflow graph instance and in the compact representation. If a path in the application workflow graph instance is not found in the latter, it is added to the compact graph. The MERGEGRAPH procedure receives the current set of vertices in the application workflow (*appVer*) and in the compact graph (*comVer*) as a parameter and, for each child vertex of the *appVer*, finds a corresponding vertex in the children of *comVer*. Each vertex in the graph has a property called *deps*, which refers to its number of dependencies. The find step considers the name of a stage and the parameters used by the stage. If a vertex is found, the path already exists, and the same procedure is called recursively to merge sub-graphs starting with the matched vertices (lines 8-9). When a corresponding vertex is not found in the compact graph, there are two cases to be considered (lines 10-23). In the first one, the searched node does not exist in *comGraph*. The node is created and added to the compact graph (lines 11-17). To check if this is the case, the algorithm verifies if the node (*v*) has not been already created and added to *comGraph* as a result of processing another path of the application workflow that leads to *v*. This occurs for nodes with multiple dependencies, e.g., D in Figure 3.2. If the path (A,B,D) is first merged to the compact graph, when C is processed, it should not create another instance of D. Instead, the existing one should be added to the children list as the algorithm does in the second case (lines 19-23). The *PendingVer* data structure is used as a look-up table to store such nodes with multiple dependencies during graph merging. This algorithm makes *k* calls to MERGEGRAPH for each *appGraphInst* to be merged, where *k* is the number of stages of the workflow. The cost of each call is dominated by the *find* operation in the

Algorithm 1 Compact Graph Construction

```
1: Input: appGraph; parSets;
2: Output: comGraph;
3: for each set  $\in$  parSets do
4:   appGraphInst = INSTANTIATEAPPGRAPH(set);
5:   MERGEGRAPH(appGraphInst.root, comGraph.root);
6: end for
7: procedure MERGEGRAPH(appVer, comVer)
8:   for each v  $\in$  appVer.children do
9:     if ( $v' \leftarrow$  find(v, comVer.children)) then
10:      MERGEGRAPH( $v, v'$ );
11:    else
12:      if (( $v' \leftarrow$  PendingVer.find(v)) ==  $\emptyset$ ) then
13:         $v' \leftarrow$  clone(v)
14:         $v'.depsSolved \leftarrow 1$ 
15:        comVer.children.add( $v'$ )
16:        if  $v'.deps \geq 1$  then
17:          PendingVer.insert( $v'$ )
18:        end if
19:        MERGEGRAPH( $v, v'$ );
20:      else
21:        comVer.children.add( $v'$ )
22:         $v'.depsSolved \leftarrow v'.depsSolved + 1$ 
23:        if  $v'.depsSolved == v'.deps$  then
24:          PendingVer.remove( $v'$ )
25:        end if
26:        MERGEGRAPH( $v, v'$ )
27:      end if
28:    end if
29:  end for
30: end procedure
```

comVer.children. The *children* will have a size of up to n or $|parSets|$ in the worst case. By using a hash table to implement children, the find is $\mathcal{O}(1)$. Thus, the insertion of n instances of the workflow in the compact graph is $\mathcal{O}(kn)$.

3.3 Task-Level Merging

In order to implement any fine-grain merging algorithm we must first address the memory and parallelism limitations. When excessive task-level merging is performed the joint number of parameters and variables may not fit on the system memory. Also, it is possible for all stages to be merged in a number smaller than the number of available nodes, hence making some of the available resources idle. Both these problems can be

solved by limiting the maximum number of stages that can be merged (bucket size). This limit is defined here as $MaxBucketSize$. Another way to enforce memory restriction is to limit the maximum number of tasks per group of merged stages (buckets). This limit is the $MaxBuckets$.

3.3.1 Naïve Algorithm

In the interest of better understanding the task-level merging problem, a naive algorithm was implemented to serve as a baseline for our analysis. This simplified algorithm groups stages in buckets of size $MaxBucketSize$ and attempt to merge all stages of each bucket among themselves. The grouping was performed by adding the stage of id i to bucket $i \bmod MaxBucketSize$. The $MaxBucketSize$ constraint was employed as a mechanism to prevent the generation of merged stages that are impossible to execute. This can happen if a bucket is big enough such that a node could not hold all the stages running concurrently (not enough memory for all arguments). We recognize that this value is of such importance that further work will be conducted to find ways to optimize it.

Although this simple solution was quickly implemented and has a linear algorithmic complexity its reuse efficiency is, however, highly dependent on the stages ordering. For instance, if similar stages were to be generated close together a greater amount of reusable computation is more likely to exist.

3.3.2 Smart Cut Algorithm (SCA)

Another strategy to create buckets of stages to be merged is through the use of a graph based representation (Figure 3.5). A representation for this could be done using fully-connected undirected graphs on which the stage instances are the nodes and each edge is the degree of reuse between two stage instances (Figure 3.5b). By degree of reuse we mean the number of tasks that would be reused if the two stages would be merged. With this perspective we would need only to partition this graph in subgraphs, maximizing the reuse degree of all subgraphs. This is a well-known problem, called min-cut [25].

Although there are many variations for the min-cut problem we define here a min-cut algorithm as one that takes an undirected graph and performs a 2-cut (i.e., cut the graph in two subgraphs) operation, minimizing the sum of the cut edges weight. This 2-cut operation was selected because of its flexibility and computational complexity. First, the recursive use of 2-cuts can break a graph in any number of subgraphs. Moreover, k-cut algorithms are not only more computationally intensive than 2-cut algorithms, but also have no guarantees for the balancement of the subgraphs (e.g., for $k = 5$ on a graph with 10 nodes one possible solution is 4 subgraphs with 1 node each and 1 subgraph with 6

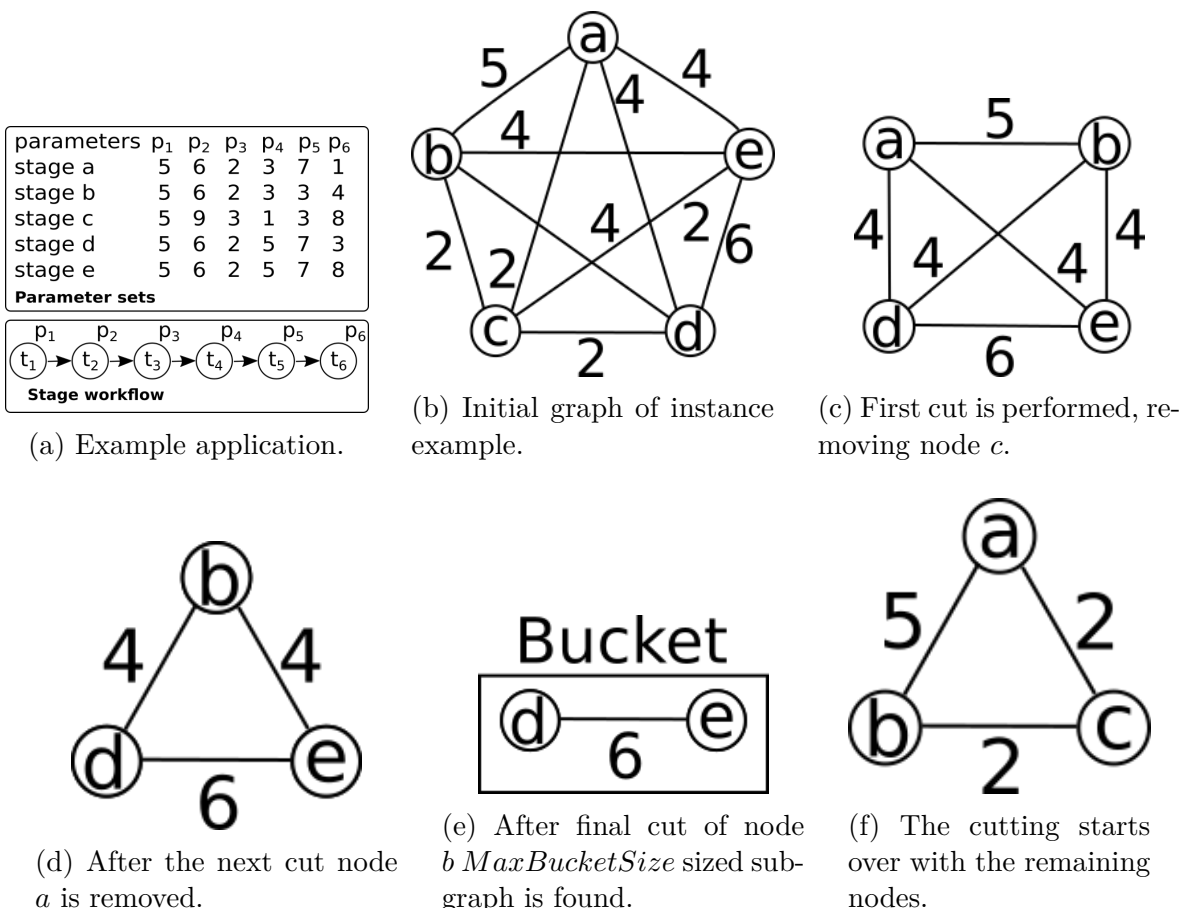


Figura 3.5: An example on which SCA executes on 5 instances of a workflow application of 6 tasks, with $MaxBucketSize = 2$.

nodes). As such, we can implement a simple k-cut balanced algorithm by performing 2-cut operations on the most expensive graph/subgraph until a stopping condition is reached (e.g., number of subgraphs is reached, number of nodes per subgraph is reached). With all these considerations only 2-cut operations are used on the proposed algorithm.

Figure 3.5 demonstrate a way to group stages into buckets using 2-cut operations. First, the fully-connected graph is generated (Figure 3.5b), given the stage instances (Figure 3.5a). Figure 3.5c shows the result of the first 2-cut operation, on which the subgraph containing only the node c is found to be the one least related to the subgraph with the remaining nodes. This is similar to the state that c is the “least reusable” stage among all other stages. Next, nodes a and b are removed until a bucket of size 2 is reached (see Figures 3.5c and 3.5d). The previously removed nodes (a , b and c) are then put together (Figure 3.5f) and the same cutting algorithm starts over. This process is then repeated until all stages are grouped into buckets.

With this procedure in mind Algorithm 2 was designed. This algorithm performs successive 2-cut operations on the graphs to divide it into unconnected subgraphs that

fit in a bucket. The cuts are performed such that the amount of reuse lost with a cut is minimized. In more detail, the partition process starts by dividing the graph into 2 subgraphs (s_1 and s_2) using a minimum cut algorithm [25] (line 4). Still, after the cut, both subgraphs may have more than $MaxBucketSize$ vertices. In this case, another cut is applied in the subgraph with the largest number of stages (lines 5-7), and this is repeated until a viable subgraph (number of stages $\leq MaxBucketSize$) is found. When this occurs, the viable subgraph is removed from the original graph (lines 8-11), and the full process is repeated until the graphs with stage instances yet not assigned to a bucket can fit in one.

Algorithm 2 Smart Cut Algorithm

```

1: Input: stages; MaxBucketSize;
2: Output: bucketList;
3: while |stages| > 0 do
4:   { $s_1, s_2$ }  $\leftarrow$  2CUT(stages)
5:   while  $|s_1| > MaxBucketSize$  do
6:     { $s_1, s_2$ }  $\leftarrow$  2CUT( $s_1$ )
7:   end while
8:   bucketList.add( $s_1$ )
9:   for each  $s \in s_1$  do
10:    stages.remove( $s$ )
11:   end for
12: end while

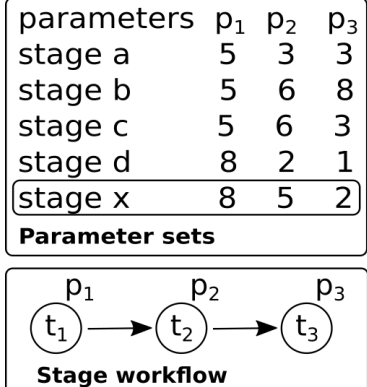
```

The number of cuts necessary to compute a single viable subgraph of n stages is $\mathcal{O}(n)$ in the worst case. This occurs when each cut returns a subgraph with only one stage and another subgraph with the remaining nodes. The cut then needs to be recomputed – about $n - MaxBucketSize$ times – on the largest subgraph until a viable subgraph is found. Also, in the worst case, all viable subgraphs would have have $MaxBucketSize$ stages and, as such, up to $n/MaxBucketSize$ buckets could be created. Therefore, the algorithm will perform $\mathcal{O}(n^2)$ cuts in the worst case to create all buckets. In our implementation, the min-cut is computed using a Fibonacci heap [25] to speed up the algorithm, making each cut $\mathcal{O}(E + V \log V)$. Since the graph used is fully connected, the complexity of a single cut in our case is $\mathcal{O}(n^2)$ and, as consequence, the full SCA is $\mathcal{O}(n^4)$. Although the SCA computes good reuse solutions, its use in practice is limited because of the computational complexity. This motivated the proposal of the strategy described in section 3.3.3.

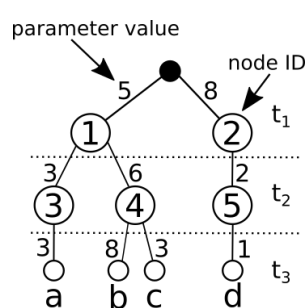
3.3.3 Reuse Tree Merging Algorithm (RTMA)

A different way of displaying the stages is in a tree structure, on which each level of the tree represents a task, and a stage s that shares a parent node on level k with s' implies

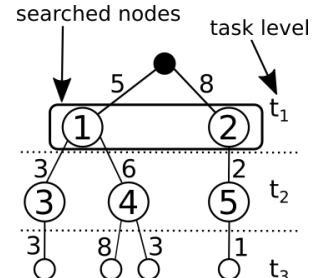
that all tasks from 1 to k are reusable among both stages. This structure is defined as a Reuse Tree, with every node being defined by its level (or height), its parent, its children and a reference to the stage responsible for its generation.



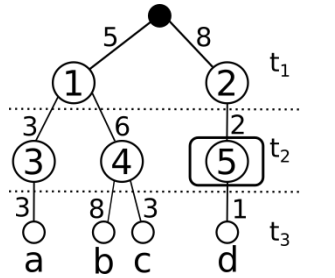
(a) Example application.



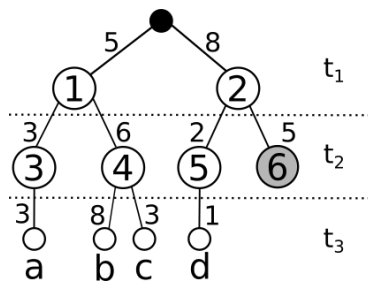
(b) Initial reuse tree for the instance example.



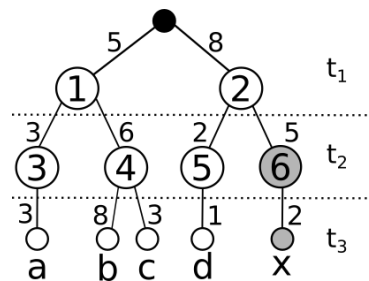
(c) Searching for reuse on the first task.



(d) Searching for reuse on the second task.



(e) Inserting a new node, 6.



(f) Inserting the leaf node x .

Figura 3.6: An example where node x is inserted on the existing reuse tree. Figure 3.6a defines the tasks of which each stage is composed by and presents the parameters' values for each stage instance.

Figure 3.6 presents an example of stage insertion (stage x) with the stage workflow and the parameters of each stage instance defined in Figure 3.6a, and the starting reuse tree in Figure 3.6b. Starting at the root node, its children (1 and 2) are searched for reuse opportunities for the first task (Figure 3.6c). Since node 2 represents all stages which task 1 has as its input $p_1 = 5$ the first task of x can be reused through it. The search for reuse for the second task is then performed on the children of node 2 (Figure 3.6d). Since node's 2 only child, node 5, cannot be reused for stage x 's second task (values for p_2 of stages d and x are different), a new node representing this non-reusable task is created (node 6) as shown in Figure 3.6e. Finally, since node 6 is new, there are no more reuse opportunities from it, thereby, a single child node must be created for each of the remaining non-reusable tasks (Figure 3.6f).

In order for a merging algorithm to be implemented on top of the Reuse Tree structure we must take advantage of its hierarchical characteristics. Given that we want to bundle

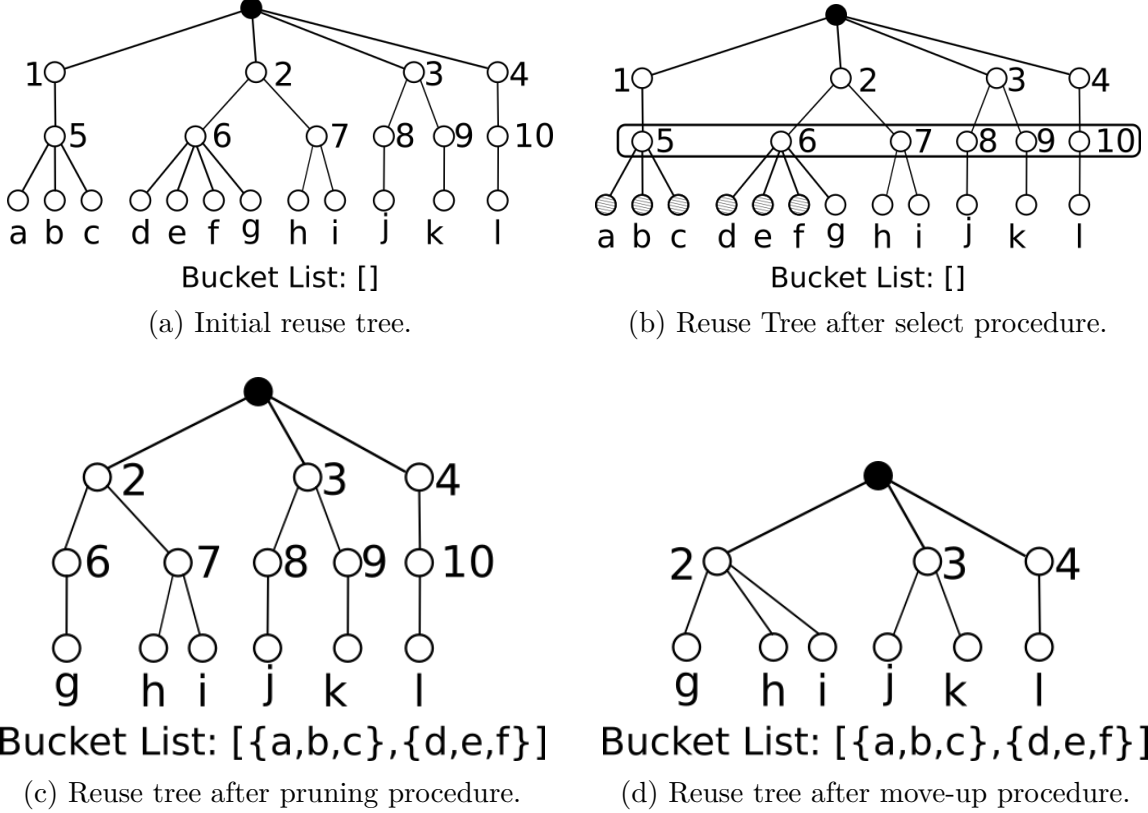


Figura 3.7: An example of Reuse Tree based merging with $\text{MaxBucketSize} = 3$. The merged stages of each step are shown below the tree on the bucket list.

together buckets of stages of at most MaxBucketSize stages we can start with the deepest stages and move up. Figure 3.7a shows an example of a Reuse Tree with 12 stages and 3 tasks each. Stages a, b and c have two out of three reusable tasks, and as such, given a $\text{MaxBucketSize} = 3$, should be put together in the same bucket. Meanwhile, stages d through i have one out of three reusable tasks. However, it is better to place three of the stages d, e, f and g together, with the remaining stage on a bucket with h and i . As we can see, the merging should happen in a bottom-up fashion.

The Reuse Tree Merging Algorithm (RTMA), listed on Algorithm 3, was implemented in three steps, (i) bucket candidates selection (line 6), (ii) tree pruning (line 7) and (iii) move-up operation (line 9), which are performed iteratively until the whole tree is consumed. If at the end of the main loop (line 5) there are still any non mergeable stages, those will be converted to one-stage buckets (lines 12-13) and then inserted on the final solution (line 14).

The first step of the algorithm (Algorithm 3, line 6) is to get a list of all leaf nodes direct parents. In Figure 3.7b we can see the selected parents (5-10). With the leaf's parents list the pruning step makes as many MaxBucketSize sized buckets as possible and then remove them from the reuse tree. The procedure *PruneLeafLevel* (line 7)

Algorithm 3 Reuse-Tree Merging Algorithm (RTMA)

```
1: Input: stages; maxBucketSize;
2: Output: bucketList;
3: bucketList  $\leftarrow \emptyset$ ;
4: rTree  $\leftarrow \text{GENERATEREUSETREE}(\text{stages})$ 
5: while rTree.height > 2 do
6:   leafsPList  $\leftarrow \text{GENERATELEAFSPARENTLIST}(r\text{Tree})$ 
7:   newBuckets  $\leftarrow \text{PRUNELEAFLEVEL}(r\text{Tree}, \text{leafsPList}, \text{maxBucketSize})$ 
8:   bucketList  $\leftarrow \text{bucketList} \cup \text{newBuckets}$ 
9:   MOVE_REUSE_TREE_UP(reuseTree, leafsPList)
10: end while
11: while rTree.root.children  $\neq \emptyset$  do
12:   newBucket  $\leftarrow \emptyset$ 
13:   newBucket.add(removeFirstChildren(rTree.root.children));
14:   bucketList  $\leftarrow \text{bucketList} \cup \text{newBucket}$ 
15: end while
16: return bucketList
```

attempts to make buckets for each leaf parent node. As stated before, the new buckets must have an exact size of MaxBucketSize , thereby, if the parent node does not have at least MaxBucketSize children it is impossible to make a bucket. Given that the parent has enough children, a number of MaxBucketSize children will be bundled together as a new bucket to later be added to the solution pool. On Figure 3.7b the two formed buckets are shown, $\{a, b, c\}$ and $\{d, e, f\}$. Each time a leaf node is added to the current new bucket, it is then removed from the parent children list, and as a consequence, removed from the tree, as seen on Figure 3.7c.

If a parent node ends up grouping all of its children in buckets, having then no more children, it must be removed from the tree (node 5 on Figure 3.7b). This process is performed recursively by removing the given childless parent node and then checking if the removal of the current parent also makes its parent childless. If this is the case the parent node removal must continue on its parent (node 1 of Figure 3.7b is also removed, as seen on Figure 3.7c).

The final step of merging is to move the leaf nodes up one level in order to enable the creation of new buckets. The operation *MoveReuseTreeUp* (Algorithm 3, line 9) is done by taking each of the previously selected parent nodes and moving all of its children to its parent's children list (e.g., nodes g, h and i of Figure 3.7c are moved to parent node 2, as seen on Figure 3.7d). After that, the current node is remove from its parent (e.g., nodes 6 and 7 of Figure 3.7c are removed from parent node 2, as seen on Figure 3.7d). After all nodes from the parent list are removed and its children are moved up the tree height is updated (line 6).

Assuming an empty tree, the *GENERATEREUSETREE* performs the insertion of n stage instances with k tasks each. In the worst case of a stage insertion there is no reuse

whatsoever, resulting in the creation of the maximum number of nodes. In this case, given that a number $m < n$ of stage instances were already added the next stage will perform m comparisons, looking for a reuse opportunity. After no opportunities are found, k nodes will be created. This results in kn new nodes generated and $n(n + 1)/2$ nodes traversed in total, and as a consequence, GENERATEREUSETREE is $\mathcal{O}(n^2)$.

The analysis of the actual merging algorithm will be split by the three operations performed on the reuse tree. Starting with the select operation, on the worst case, there will be one child per stage (i.e., no reuse on the first task), resulting in n nodes visited. On this case, the number of children of each node beyond the first level will be one, resulting in $k - 2$ extra nodes visited. As a result we have that that *GenerateLeafsParentList* runs in $\mathcal{O}(nk)$ per iteration, or $\mathcal{O}(nk^2)$, for there are exactly $k - 1$ iterations.

For the pruning step the most expensive operation is the one of adding a stage to a solution bucket. Knowing that the exact number of bucket insertions must be at most n for the whole merging algorithm, we get the complexity $O(n)$ for all iterations of the pruning step.

At last, the complexity of the move-up step will be calculated by the amount of times a leaf node is moved from the current node child list to its parent. Independently to the structure of the tree, given that it has n leaf nodes, all of them will be moved once per move-up operation. Given that there are exactly $k - 1$ iterations, we have $\mathcal{O}(nk)$.

The RTMA complexity is then dominated by tree generation algorithm since it's $\mathcal{O}(n^2)$, versus the joint complexity of the other three steps, $\mathcal{O}(nk^2 + nk + n)$. This happens because $n \gg k$ by the order of hundreds to thousands times greater. With such time complexity, the RTMA is expected to scale enough in order to be a viable solution.

3.3.4 Task-Balanced Reuse Tree Merging Algorithm (TRMA)

Given the nature of the chosen SA application and its scale (both computational cost and used resources wise), unbalance issues cannot, on most cases, impact the overall performance of the RTMA. However, there may exist cases on which balance may become a problem to be solved. This is the case when the ratio of buckets per computing node (or core) is low. Although the threshold of how low it must be in order to impact the makespan of the application can only be determined empirically, this problem cannot be ignored. As such, a balanced version of RTMA was implemented, the Task-Balanced Reuse Tree Merging Algorithm (TRMA).

The TRMA can be explained as an improved version of the RTMA, on which the balance of the buckets' cost is taken into consideration. This is achieved by breaking all stages into an user-defined number of buckets, which are balanced afterwards. This balance is task-wise, meaning that the difference of task number of any two buckets

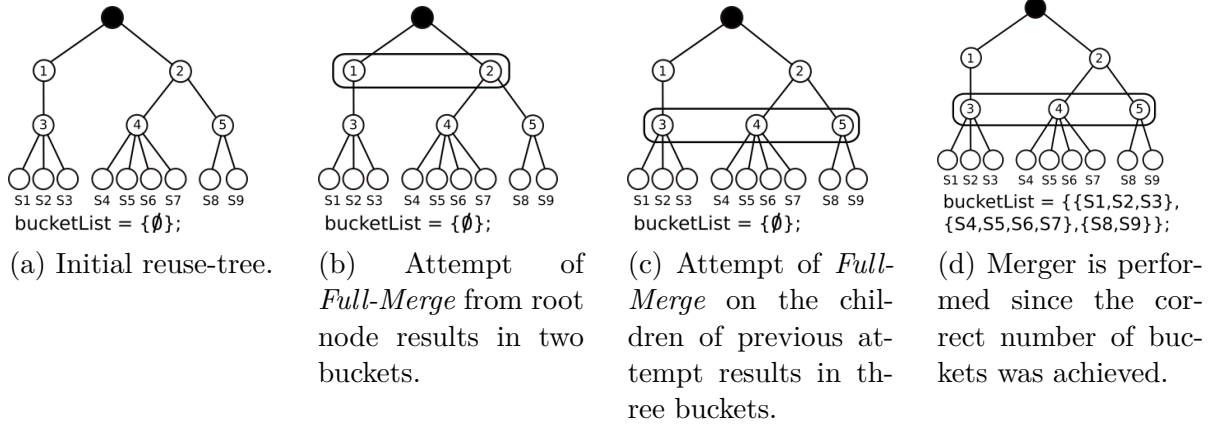


Figura 3.8: Simple example of *Full-Merge* on which *MaxBuckets* is 3 and the exact division os stages is reached.

at the end of the TRMA is at most k , being k the number of tasks that a stage is composed. Although we cannot ensure that the computational cost of all types of tasks are equivalent, being this another source of unbalance, the granularity of unbalance is smaller, resulting in a better result, when comparing with the previous approaches covered by this work.

The TRMA is performed in three steps, using the same reuse-tree structure as the one used by the RTMA. At first, all stages are divided into *MaxBuckets* disjoint buckets that maximizes the overall reuse, in an operation defined as *Full-Merge*. This means that there cannot exist another combination of disjoint buckets which has an overall cost (total number of non-repeated tasks) smaller than the set of buckets outputted by the *Full Merge* operation. Figure 3.8 shows an example of the *Full-Merge* process on which the stages are perfectly divided into the three buckets. As seen in Figure 3.8d, after the stopping condition of *Full-Merge* the stages are arranged in buckets, while preserving the reuse-tree for further use (i.e., balancing).

Still, there may be a case on which the *Full-Merge* will not be able to exactly divide the stages in *MaxBuckets*. On this particular case, as shown in Figure 3.9, the *Full-Merge* operation will stop then the number of buckets is greater than *MaxBuckets*, as seen in Figure 3.9b. From this number of buckets greater than *MaxBuckets* another merger process is applied, the *Fold-Merge*.

It is simple to notice that for a set of ordered numbers (sized n , being n even) which we want to find set of $n/2$ disjoint pairs of distinct numbers that minimizes the maximum sum of each pair, we can simply pair the opposite ends of the initial set. E.g., for a set $\{1,2,3,4,5,6\}$ we can have the result set $\{\{1,6\}, \{2,5\}, \{3,4\}\}$, in a procedure that resembles a visual “folding” of the initial set, pivoted on the center of the list (between 3 and 4).

As such, we want to transform a set of n buckets in another set of size *MaxBuckets*

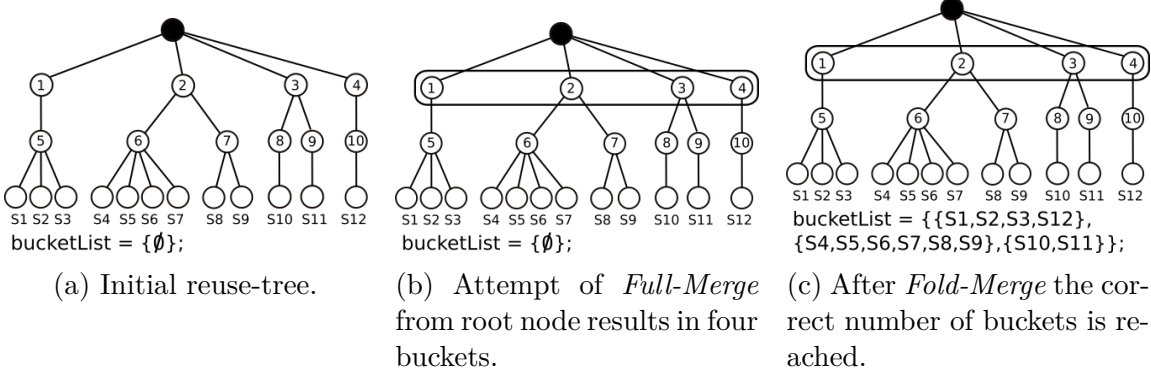


Figura 3.9: Another example of *Full-Merge* and *Fold-Merge* on which *MaxBuckets* is 3 and the exact division of stages cannot be reached by *Full-Merge*.

$(n > \text{MaxBuckets})$, which can be achieved by performing a “folding” operation on $k = 2(n - \text{MaxBuckets})$ buckets. The k “folded” buckets are selected in order to minimize the maximum cost of the *MaxBuckets* output buckets, being the cost defined by the number of different tasks of a buckets. Thus, the k buckets with the smallest cost are chosen to be “folded”. This process of folding k buckets in order to achieve *MaxBuckets* buckets is defined as *Fold-Merge*, with an example of its application shown in Figure 3.9c

With the correct number of buckets, these are then balanced among each other, on a *Balance* step, defined by Algorithm 4. An example of this operation is seen on Figure 3.10. At first, we have a reuse-tree which had its stages divided into three buckets (Figure 3.10a) as a result of the *Full-Merge* and *Fold-Merge* operations. As before, the cost of a bucket is defined by the number of different tasks it has. As stated on Algorithm 4, we attempt to balance the buckets represented by the reuse-tree nodes with greatest (*bigRTN*) and smallest (*smallRTN*) costs of all input buckets (*bucketList*). It is worth noting that although the input data structure of *Balance* is a list of buckets, each one of its stages are also leaf nodes of the reuse-tree generated by the previous steps of the TRMA.

An attempt of balancement is defined as a reuse-tree node $\text{improvement} \in \text{bigRTN}$, which leaf nodes can be subtracted from subtree *bigRTN* and added to subtree *smallRTN*, resulting in a smaller unbalance value, i.e., being $\text{unbal} = \text{TaskCost}(\text{bigRTN}) - \text{TaskCost}(\text{smallRTN})$ the old unbalance and $n\text{Unbal} = \text{Max}(\text{TaskCost}(\text{bigRTN} \setminus \text{improvement}) - \text{TaskCost}(\text{smallRTN} \cup \text{improvement}))$ the new unbalance value, $\text{unbal} < n\text{Unbal}$. Also, in order for a balancement improvement be valid the new maximum cost value, after the improvement, must be smaller than *bigRTN* cost. This constraint prevents useless balancement attempts, i.e., the unbalance value is improved but there is no difference in the application makespan. An example of useless improvement can be seen in Figure 3.10d, on which the improvement of sending the chil-

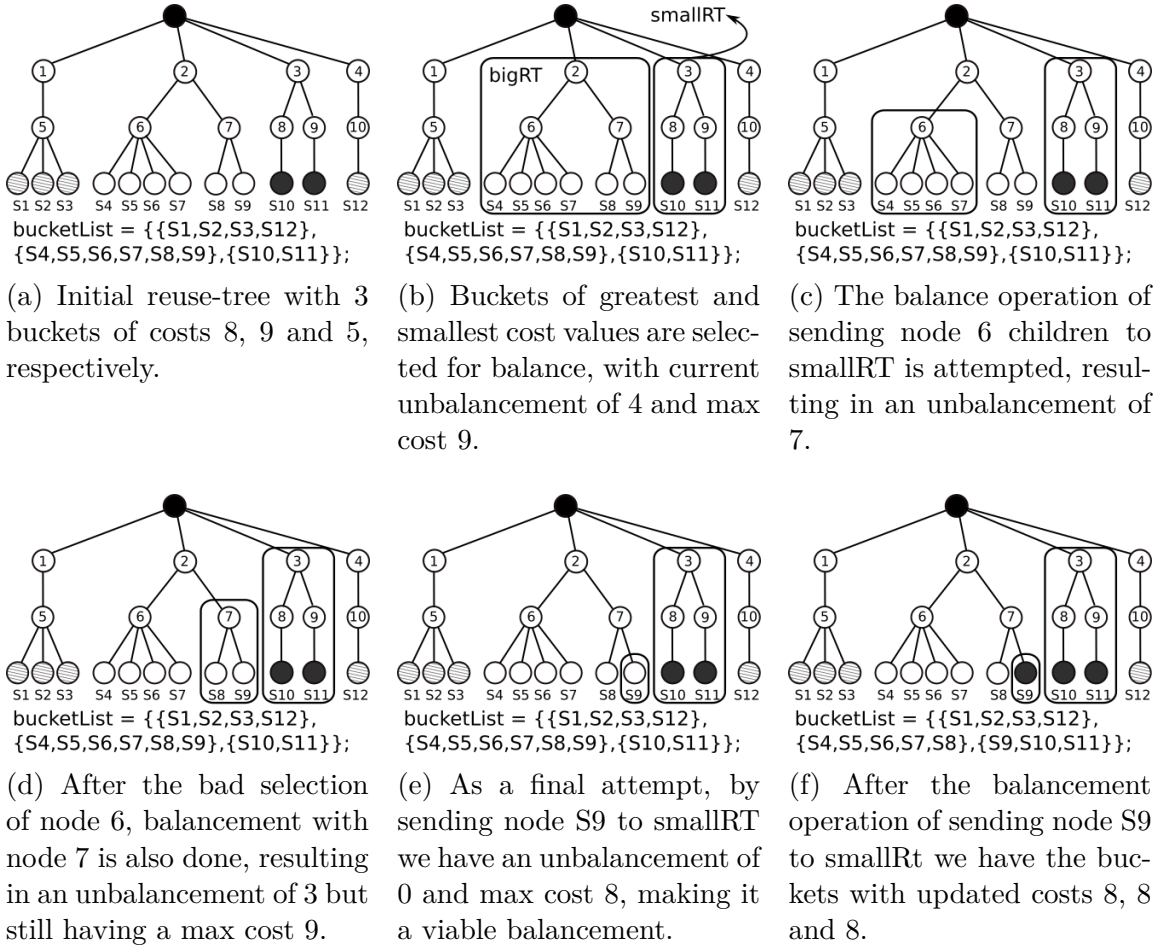


Figura 3.10: An example of the *Balance* step on which there are 3 buckets to be balanced.

dren of node 7 to smallRTN, represented by node 3, results in a better unbalance (3 vs the previous 4) while not improving the final outcome of the balance procedure (the maximum cost of the buckets under balance is still 9). We call this an unnatural improvement, on which a better balance value is achieved by simply increasing the cost of *smallRTN*, thus, not having any positive contribution to the application makespan. This check is performed at lines 9 and 10 of Algorithm 4.

The process of finding balance attempts is demonstrated on Algorithm 5. It starts with two input subtrees, *bigRTN* and *smallRTN*, being the first, the one with the greatest cost. As shown in lines 4 and 10 of Algorithm 5, the search is performed in a depth first search fashion, on which every visited node (*c*) is checked as an improvement (lines 5-9). If there is not any improvements on *bigRTN*, \emptyset is returned (lines 3 and 16).

This search process is exemplified on Figure 3.10. Given the selected *bigRTN* and *smallRTN* on Figure 3.10b, the nodes of *bigRTN* are searched for improvements. On Figure 3.10c, on which node 6 is visited, the attempt of sending stages S4-S7 to *smallRTN* results in *bigRTN* with cost 4 and *smallRTN* with a new cost of 11. Given that this is

Algorithm 4 The *Balance* step of the TRMA

```
1: Input: bucketList;
2: Output: bucketList;
3: while true do
4:   sort bucketList by descending cost
5:   bigRTN ← bucketList.first()
6:   smallRTN ← bucketList.last()
7:   unbal ← TaskCost(bigRTN) - TaskCost(smallRTN)
8:   improvement ← SingleBalance(bigRTN, smallRTN, unbal)
9:   newMksp ← Max(TaskCost(bigRTN \ improvement), TaskCost(smallRTN ∪ improvement))
10:  if improvement ≠ ∅ and newMksp < TaskCost(bigRTN) then
11:    smallRTN ← smallRTN ∪ improvement
12:    bigRTN ← bigRTN \ improvement
13:  else
14:    break
15:  end if
16: end while
17: return bucketList
```

not an acceptable balancement attempt the current best improvement value continues to be \emptyset . After that, node 7 is searched (Figure 3.10d). On this case we have a better unbalance, validating it as an improvement (although, being an unnatural improvement), then becoming the new best solution (Algorithm 5, lines 7 and 8). Finally, one of the leaf nodes is searched, resulting in a task cost of 8 for both $bigRTN$ and $smallRTN$, and as such, an unbalance of 0 (Figure 3.10e). After the search for balancement attempts between $bigRTN$ and $smallRTN$ is finished, the current best solution (leaf node S9) is tested by Algorithm 4 (lines 10-12) and accepted. Since there cannot be an improvement on the current unbalance of 0, the next attempt of *SingleBalance* (line 8) will return an $improvement = \emptyset$, thus ending the *Balance* step.

Algorithm 5 Balancement algorithm for two tree nodes (*SingleBalance*)

```
1: Input: bigRTN; smallRTN; unbal;
2: Output: improvement;
3: improvement ← ∅
4: for each unique children c ∈ bigRTN do
5:   newUnbal ← | TaskCost(bigRTN \ c) - TaskCost(smallRTN ∪ c) |
6:   if newUnbal < unbal then
7:     unbal ← newUnbal
8:     improvement ← c
9:   end if
10:  bestRec ← SingleBalance(c, smallRTN, unbal)
11:  if bestRec ≠ ∅ then
12:    unbal ← | TaskCost(bigRTN \ bestRec) - TaskCost(smallRTN ∪ bestRec) |
13:    improvement ← bestRec
14:  end if
15: end for
16: return improvement
```

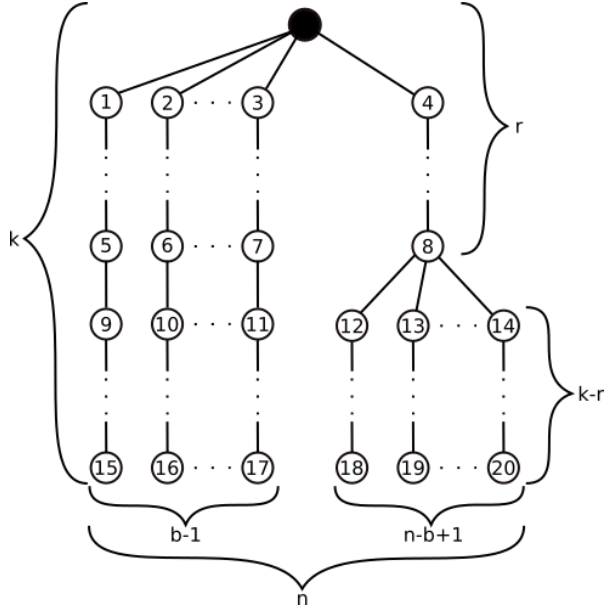


Figura 3.11: A general worst-case reuse-tree representation on which we have all n stages divided into b buckets. On this case we have $b - 1$ buckets with exactly one stage, and thus cost k . Hence, the last bucket has $n - b + 1$ stages. For this last bucket we assume the single and uniform reuse of the first r task, having no reuse for the remaining $k - r$ tasks. This is the worst-case for balancement applications.

Given the already known complexity for the reuse-tree generation, of $\mathcal{O}(n^2)$, the *Full-Merge*, *Fold-Merge* and *Balance* operations remain to be analyzed. On the worst case *Full-Merge* will visit every node of the reuse-tree. Since there cannot be more than kn nodes on a reuse-tree, being k the number of tasks of each one of the n stages, the complexity for *Full-Merge* is bounded by $\mathcal{O}(kn)$. Moreover, the necessary calculations for *Fold-Merge* can be performed in constant time, and that we have b buckets to look into, the computational cost for this operation is negligible. Given that these two operations are less expensive than the reuse-tree generation procedure, their cost are ignored.

In order to calculate the complexity for the remaining operation, *Balance*, we must first create a general model for a worst-case reuse-tree, which is seen in Figure 3.11. On this model, we have a reuse-tree divided into b buckets, of which $b - 1$ have exactly one stage. This represents a worst-case scenario on which one big bucket is shrinked one stage at a time, until a perfect balance is achieved. E.g., given 3 buckets B_1 , B_2 , and B_3 , with respectively 1, 1 and 4 stages, and with all the stages of B_3 having the first task reusable among all 4 stages, the costs for the 3 buckets will be 2, 1, 3 after the first balance iteration, and 2, 2, 2 after the second iteration.

Furthermore, *Balance* is divided into two main parts, the main loop of Algorithm 4, and the balancement attempts of Algorithm 5. The main loop of *Balance* runs while there

are improvements, which value can be estimated using the general model of Figure 3.11. Since the last bucket (beginning on node 4) has $n - b + 1$ stages and it will reach perfect balance once its size reaches n/b we have that $n - b + 1 - n/b$ improvement operations will be performed. Besides, for each improvement attempt there will be a call to the algorithm used for sorting the buckets by their cost (Algorithm 4, line 4) and a call for **SINGLEBALANCE**. Seeing that on the worst case **SINGLEBALANCE** will visit each node of the biggest bucket (i.e., the last bucket of Figure 3.11, represented by node 4), totalizing $r + (n - b + 1)(k - r)$ nodes, and also that, generally, good sorting algorithms are $\mathcal{O}(n \log(n))$, we arrive at the final complexity of $\mathcal{O}(kn^2 + nb \log(b))$. Similarly to the RTMA, $n \gg k$, ergo, the time complexity can be dominated by n^2 . In the same manner, if the number of buckets is large enough it approaches $n^2 \log(n)$. This case is, however, unlikely, since it means that for n stages we want to separate them in n to n/b ($b \simeq n$ and $n > b$) buckets, resulting in a speedup of at most n/b , which does not justify the use of any fine-grain merging algorithm. This speedup is calculated based on the best case scenario, on which there is maximum reuse on every bucket, e.g., a bucket with 5 stages and k tasks per stage has $k + 4$ tasks.

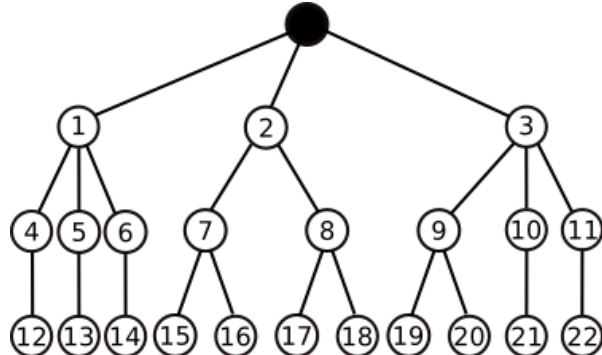


Figura 3.12: An example reuse-tree that can be used to illustrate possible prunable nodes. E.g., the use of nodes 4, 5, 6, or 10, 11 as an improvement attempt results in the same outcome (cost 3), making them interchangeable, as with nodes 7, 8 or 9 (cost 4), or nodes 12-22 (cost 3).

As a final observation, it is easy to notice that any leaf node on the interval of S4-S9 of Figure 3.10e would result in the same balancement outcome (an unbalance of 0 with all buckets with cost 8). As such, it would be interesting if we pruned all nodes that would result in the same outcome. This can be, and is, achieved by verifying both the number of children and the cost of two nodes. If both values are the same than we have similar (or non-unique) nodes, meaning that only one of the nodes must be searched. This strategy is currently implemented locally, meaning that only sibling nodes are verified, which can be seen using Figure 3.12.

By verifying prunable nodes locally it is meant that a node can only be pruned if the equivalent (repeated) search node is a sibling. On Figure 3.12 this means that when searching the children of node 1, only node 4 would be further searched, being node 12 searched afterwards, ignoring nodes 5 and 6. As the search progresses, on the search of the children of node 2, only the nodes 7 and 15 would also be searched. Finally, nodes 9 and 10, and their children would be searched as well. However, by keeping a list of searched nodes, uniquely ordered by their children count and overall cost, it is possible to extend this strategy to a global scope, thus removing the sibling-only prunable node restriction. While using local prune on the reuse-tree of Figure 3.12 would result in the search of 11 nodes (1, 4, 12, 2, 7, 15, 3, 9, 19, 10 and 21), a global prune scheme would result in 7 nodes searched (1, 4, 12, 2, 7, 15, 3).

In order to implement a global scope prune algorithm there is the need for both children count and overall cost metrics. Assuming that the reuse-tree of Figure 3.12 does not have the subtree of node 3, both subtrees of nodes 1 and 2 would have the same overall cost (6). Thus, by considering only the overall cost, subtree 2 would not be searched, resulting in the missed opportunity of balancing with subtree 7 which has a cost of 4 (from the root node), an impossible value to achieve with only subtree 1 (which can achieve a costs 3 with nodes 1, 4 and 12, or 5 with nodes 1, 4, 12, 5 and 13). Likewise, by only verifying the children count on a reuse-tree with only the subtrees of nodes 1 and 3 we would come to the same fallacy of pruning a necessary subtree (this time, subtree of node 3), hence, making it necessary the use of both metrics.

Capítulo 4

Experimental Results

This chapter presents the experimental results of all proposed algorithms of the previous chapter, regarding scalability, bucket cost balancement, the impact of different Sensitivity Analysis methods on reuse and the impact of the bucket size on run time.

4.1 Experimental Environment

We evaluated the proposed algorithms using a set of tissue images from brain cancer studies [14]. The images were divided into $4K \times 4K$ tiles for concurrent execution. The image analysis workflow consisted of normalization, segmentation and comparison stages. The comparison stage computes the difference between masks generated. The experimental evaluations were conducted on a distributed memory machine, the TACC Stampede cluster. Each node has dual socket Intel Xeon E5-2680 processors, an Intel Xeon Phi SE10P co-processor and 32GB RAM. The nodes are inter-connected via Mellanox FDR Infiniband switches. Stampede uses a Lustre file system accessible from all nodes. The application and middleware codes were compiled using Intel Compiler 13.1 with “-O3” flag.

4.2 Impact of Multi-level Computation Reuse and SA methods

This section presents the impact of the computation reuse to the performance for the MOAT and VBD SA methods. We first compute MOAT on all the application parameters, because it demands a smaller per parameter sampling to exclude those parameters that are non-influential to the output from the VBD. Most of the experiments in this section were executed using a small number of machines, because this section intended to detail

the gains with the reuse optimizations. However, Section 4.3 presents the results for runs with a large number of nodes in which the gains with the computation reuse optimization remain the same.

4.2.1 Impact of Multi-level Computation Reuse for MOAT

Figure 4.1 presents the execution times of MOAT studies with parameter sample sizes varying from 160 to 640, which were executed using only 6 nodes to demonstrate the impact of the optimizations. The parameters were generated with a quasi-Monte Carlo sampling using a Halton sequence, which is known to provide a good coverage of the parameter space. These experiments use *maxBucketSize* set to 7, and the execution times refer to the makespan and include the cost to perform the computation reuse analysis. For the task level merging approaches, the time spent by the merging algorithm is shown in the upper part of the graph bars. Additionally, five application versions were executed: the “No reuse” that employs the replica based composition, the “Stage level” performs reuse only of stage instances, and the “Task Level” that reuses fine-grain tasks and is executed with the Naïve, SCA, and RTMA algorithms.

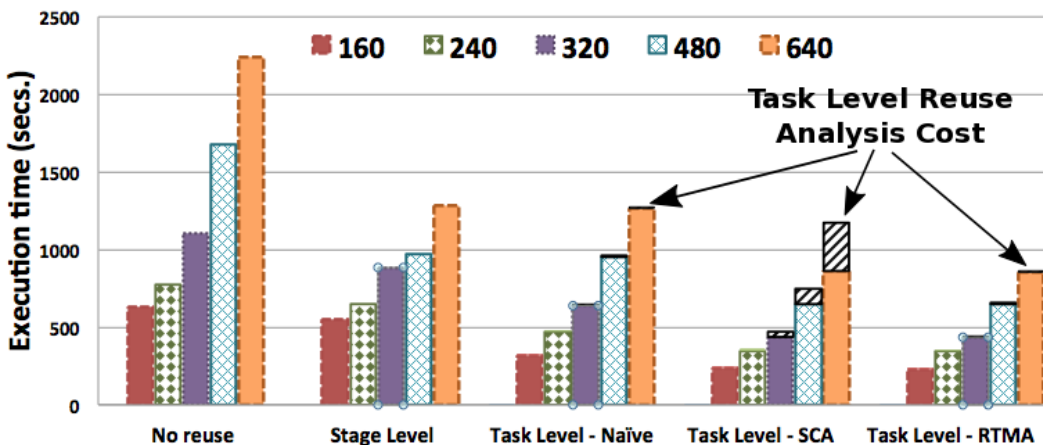


Figura 4.1: Impact of the computation reuse for different strategies as the sample size of the MOAT analysis is varied.

The results presented in Figure 4.1 show that all application versions that reused computation significantly outperformed the baseline “No reuse” version. The Stage Level reached a speedup of up to $1.85\times$ on top of the No reuse, while the application versions with Task Level reuse have higher gains. The Task Level Naïve is only slightly better than the Stage Level ($1.08\times$ faster in the best case). This result is attributed to the highly order dependent nature of the naïve approach. The Task Level with SCA and RTMA, on

the other hand, have remarkable speedups of up to, respectively, $1.39\times$ and $1.5\times$ on top of the Stage Level reuse only.

It is also noticeable from Figure 4.1 that the performance gains with RTMA increase as the sample size grows as a consequence of more reuse opportunities. In the SCA algorithm however, the opposite behavior is observed. This is a result of the higher costs of executing SCA to compute the stages to be merged, as expected, which offsets the gains with the actual execution of the application after the merging. The time taken by Naïve, SCA, and RTMA to compute the reuse are shown on the top of their bars on Figure 4.1. For a sample of size 640, the time taken by SCA is about 26% of the entire execution. It is also interesting to see that although the RTMA takes a much shorter time to compute the merging choices, and provides better solutions than SCA. In the best case, RTMA attained a speedup of up to $2.61\times$ on top of the “No reuse” version.

4.2.2 Impact of Multi-level Computation Reuse for VBD

The performance of the proposed optimizations for the VBD are presented in Figure 4.2. The VBD was executed using the remaining 8 parameters (the original parameter set contains 15 parameters) that were not discarded in the MOAT analysis. VBD requirements are of the order of hundreds to thousands runs per parameter. As such, the sample size in this experiment is higher and was varied from 2000 to 10000 runs, whereas the same application versions used with MOAT were evaluated. In order to accelerate this analysis, we have increased the number of nodes to 16.

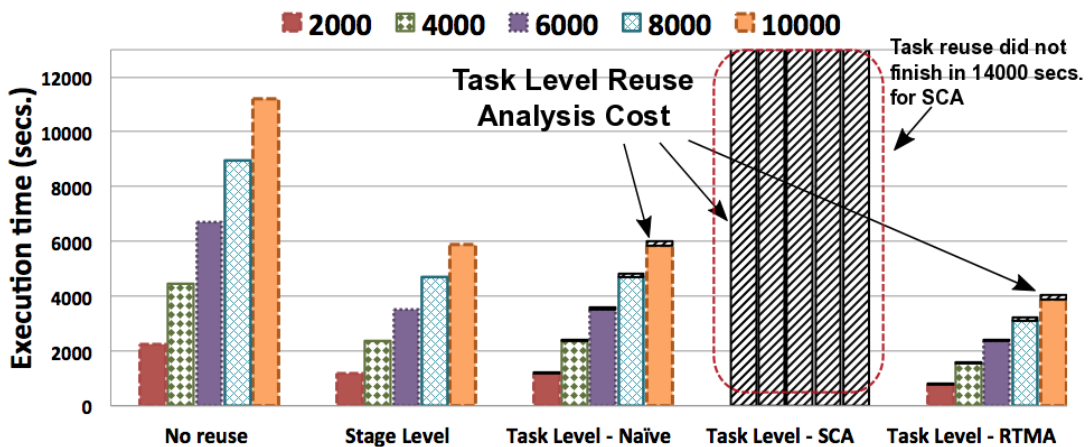


Figura 4.2: Impact of the computation reuse strategies for the VBD SA method.

As presented in Figure 4.2, the relative performance of the application versions is similar to that observed with MOAT, except for the task level merging using SCA. Given

that the sample size used in VBD is much higher, the SCA was not even able to finish computing the reuse and begin executing the workflow in 14000 secs.

4.3 Impact of Bucket Size and Its Effect on Parallelism

Figure 4.3 additionally presents the impact of varying the *maxBucketSize* size to the execution times. As expected, the increase in *maxBucketSize* leads to smaller execution times because of the larger number of merging opportunities. However, it is interesting to notice that the variation in execution times as a result of the bucket size changes is up to 12%, which shows that the Task Level reuse can achieve significant gains even with small bucket sizes. Finally, in a large-scale SA using with sample size of 240, 4,276 4K×4K image tiles, and 128 computing nodes, using all optimizations and the No reuse, Stage Level, and Task Level RTMA versions of the workflow attained execution times of, 15,681s, 12,544s and 6,173s, respectively.

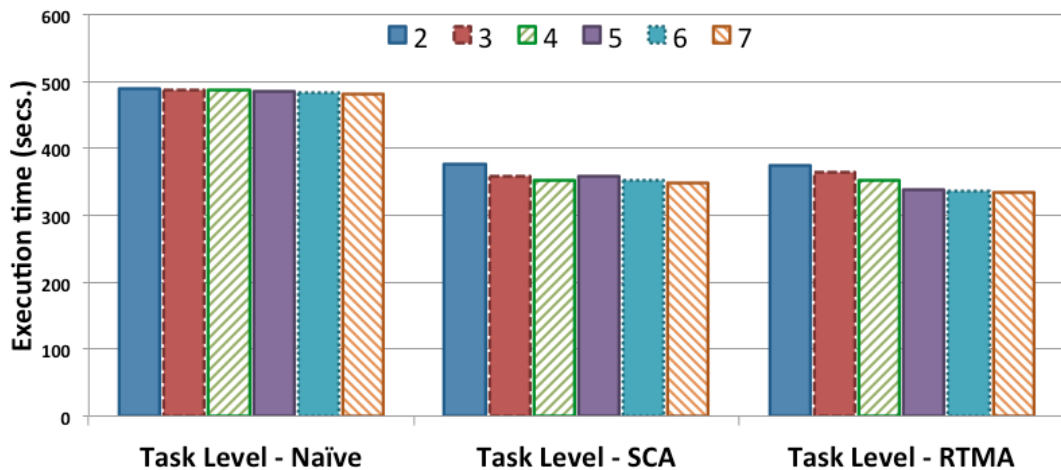


Figura 4.3: Impact of varying *MaxBucketSize*.

We want to highlight that the task level merging reduces the number of stage instances in up to *maxBucketSize* and, as a consequence, the parallelism. This could affect the application scalability if the number of stage instances after the merging was not sufficient to completely use the parallel environment. However, this is not the case in a large-scale SA, because the number of stages instances to be executed in a study is very high. For instance, a SA with a sample size of 240 and 4,276 4K×4K image tile, as employed in the previous experiment, involves the execution of $240 \times 4276 \times 3$ (stages) or about 3×10^6 stage instances. Its reduction by *maxBucketSize* during the merging will still lead to

a configuration with sufficient stage instances to use the environment in the scale we are running (up to 256 nodes). We have experimentally validated it, and the scalability before and after merging has no significant difference when up to 256 nodes are used. We recognize, however, that if we continue to reduce the stage per node ratio, by either heavily increasing the number of nodes or reducing the number of executed stages, smaller values of *maxBucketSize* should be chosen, considering its impact into the parallelism.

4.4 Worst-Case Scalability Analysis

Given that the RTMA could not take balancement issues into consideration it was expected that there may exist some cases on which its use would result in such unbalance that even the use of coarse-grain-only reuse would be better. One of this cases was found by using the VBD SA method with a sample size of 200 (i.e., around 2000 executions) and varying the number of nodes (each one with 28 cores) from 1 to 8, or 28 to 224 cores. This comparison can be seen in Figure 4.4. RTMA used *MaxBucketSize* of 10 while TRMA used *MaxBuckets* as $2 \times \text{NumberOfCores}$, resulting in a static 2 stages per core for all node configurations.

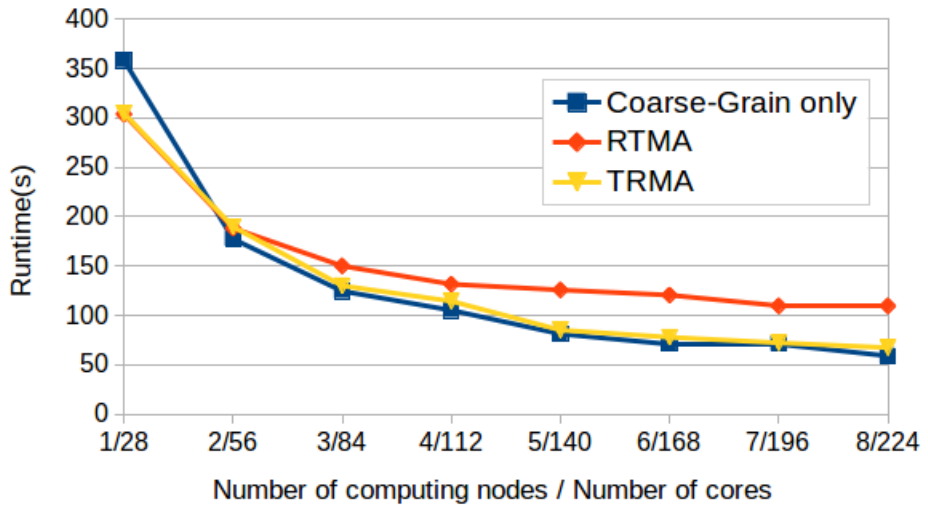


Figura 4.4: Comparison of the Coarse-grain-only approach with the RTMA and TRMA.

The results of Figure 4.4 can be split in three moments. The first one, when the number of cores is at most 56, the number of stages per core is still high enough for RTMA to avoid unbalance issues. At this time, both RTMA and TRMA have similar performances. As we move further, when the number of cores is between 56 and 112, RTMA's scalability starts to drop as TRMA and Coarse-grain only keep scaling. It is worth noting that on this interval the experimental values of TRMA and Coarse-grain only are equivalent

with a degree of confidence of 90%. The final range, with the number of cores of at least 140 shows RTMA runtime reaching a limit, given its unbalance. As for TRMA and Coarse-grain, their equivalence now reaches a degree of confidance of 95%, thus showing that the TRMA can achieve the same reuse optimization of RTMA when the issue of unbalance is nonexistent (i.e., large scale of experiments / executions) while not degrading it's performance on these extreme low-scale settings (low number of stages per cores).

Capítulo 5

Schedule

This chapter portraits the planning of all future activities. Below is the table with all tasks to be completed, their expected time to be completed and when they will begin:

Activity/Month	2017											2018	
	03	04	05	06	07	08	09	10	11	12	01	02	
Attend Seminaries course	•	•	•	•	•								
Attend Individual Work	•	•	•	•	•								
Elaboration course													
Perform large scale testing	•	•	•	•	•		•	•	•				
Implement the <i>MaxBucketSize</i> selection algorithm			•	•									
Optimize the reuse tree merging algorithm				•	•								
Research clustering algorithms						•	•	•					
Implement clustering-based merging algorithm							•	•					
Comparison of merging algorithms								•	•				
Write journal paper									•	•	•		
Write dissertation				•	•	•	•	•	•	•	•		
Final presentation												•	

Tabela 5.1: Schedule of activities for 2017.

Referências

- [1] Barreiros, Willian, George Teodoro, Tahsin Kurc, Jun Kong, Alba C. M. A. Melo e Joel Saltz: *Parallel and Efficient Sensitivity Analysis of Microscopy Image Segmentation Workflows in Hybrid Systems.* páginas 25–35. IEEE, setembro 2017, ISBN 978-1-5386-2326-8. <http://ieeexplore.ieee.org/document/8048914/>, acesso em 2017-11-10. x, 5
- [2] Bradski, G.: *The opencv library.* Dr. Dobb's Journal of Software Tools, 2000. 9
- [3] Campolongo, F., J. Cariboni e A. Saltelli: *An effective screening design for sensitivity analysis of large models.* Environmental Modelling & Software, 22(10):1509–1518, 2007. 1
- [4] Cooper, L., D. Gutman, Q. Long, B. Johnson, S. Cholleti, T. Kurc, J. Saltz, D. Brat e C. Moreno: *The proneural molecular signature is enriched in oligodendrogiomas and predicts improved survival among diffuse gliomas.* PloS ONE, 5, 2010. 5
- [5] Cooper, L. A., J. Kong, D. A. Gutman, F. Wang, J. Gao, C. Appin, S. Cholleti, T. Pan, A. Sharma, L. Scarpase, T. Mikkelsen, T. Kurc, C. S. Moreno, D. J. Brat e J. H. Saltz: *Integrated morphologic analysis for the identification and characterization of disease subtypes.* J Am Med Inform Assoc., 19(2):317–323, 2012. 5
- [6] Filippi-Chiela, E. C., M. M. Oliveira, B. Jurkovski, S. M. Callegari-Jacques, V. D. da Silva e G. Lenz: *Nuclear morphometric analysis (nma): Screening of senescence, apoptosis and nuclear irregularities.* PloS ONE, 7, 2012. 5
- [7] Gurcan, M. N., H. Shimada T. Pan e J. Saltz: *Image analysis for neuroblastoma classification: segmentation of cell nuclei.* Conf Proc IEEE Eng Med Biol Soc, páginas 4844—4847, 2006. 5
- [8] Han, J., H. Chang, G. V. Fontenay, P. T. Spellman, A. Borowsky e B. Parvin: *Molecular bases of morphometric composition in glioblastoma multiforme.* 9th IEEE International Symposium on Biomedical Imaging, páginas 1631–1634, 2012. 5
- [9] Iooss, B. e P. Lemaitre: *A review on global sensitivity analysis methods.* In G. Dellino and C. Meloni, editors, *Uncertainty Management in Simulation-Optimization of Complex Systems*, 59:101–122, 2015. 7
- [10] Iooss, B. e P. Lemaitre: *A review on global sensitivity analysis methods in Uncertainty Management in Simulation-Optimization of Complex Systems*, volume 59. Springer US, 2015. 1

- [11] J. Goecks, A. Nekrutenko, J. Taylor: *Galaxy: a comprehensive approach for supporting accessible, reproducible, and transparent computational research in the life sciences*. Genome Biol., 11(8), 2010. 2, 11, 12
- [12] Jr., Eugene Santos e Eunice E. Santos: *Effective computational reuse for energy evaluations in protein folding*. International Journal on Artificial Intelligence Tools, 15(5):725—739, 2006. 2, 11, 12
- [13] Kong, J., L. A. D. Cooper, F. Wang, J. Gao, G. Teodoro, T. Mikkelsen, M. J. Schniederjan, C. S. Moreno, J. H. Saltz e D. J. Brat: *Machine-based morphologic analysis of glioblastoma using whole-slide pathology images uncovers clinically relevant molecular correlates*. PLoS ONE, 2013. 1
- [14] Kong, Jun, Lee A. D. Cooper, Fusheng Wang, Jingjing Gao, George Teodoro, Tom Mikkelsen, Matthew Schniederjan J., Carlos S. Moreno, Joel H. Saltz e Daniel J. Brat: *Machine-based morphologic analysis of glioblastoma using whole-slide pathology images uncovers clinically relevant molecular correlates*. PLoS ONE, 2013. 33
- [15] Körbes, A., G. B. Vitor, R. de Alencar Lotufo e J. V. Ferreira: *Advances on watershed processing on gpu architecture*. In Proceedings of the 10th International Conference on Mathematical Morphology, 2011. 5
- [16] Meredith, J. S., S. Ahern, D. Pugmire e R. Sisneros: *Eavl: The extreme-scale analysis and visualization library*. páginas 21–30, 2012. 5
- [17] Mood, Benjamin, Debayan Gupta, Kevin Butler e Joan Feigenbaum: *Reuse it or lose it: More efficient secure computation through reuse of encrypted values*. Proceedings of the 2014 ACM SIGSAC Conference on Computer and Communications Security, páginas Pages 582–596, 2014. 2, 10, 12
- [18] Morris, M. D.: *Factorial sampling plans for preliminary computational experiments*. Technometrics, 33(2):161–174, 1991. 1, 7
- [19] Nakra, T., R. Gupta e M. Soffa: *Value prediction in vliw machines*. Int. Symp. Computer Architecture, páginas 258–269, 1999. 2, 10
- [20] Patlolla, D. R., E. A. Bright, J. E. Weaver e A. M. Cheriyadat: *Accelerating satellite image based large-scale settlement detection with gpu*. In Proceedings of the 1st ACM SIGSPATIAL International Workshop on Analytics for Big Geospatial Data, páginas 43–51, 2012. 5
- [21] Richardson, S. E.: *Caching function results: Faster arithmetic by avoiding unnecessary computation*. Technical Report, Sun Microsystems Laboratories, 92(1), 1992. 2, 10, 11, 12
- [22] Saltelli, A. (editor): *Global sensitivity analysis: the primer*. John Wiley, Chichester, England ; Hoboken, NJ, 2008, ISBN 978-0-470-05997-5. OCLC: ocn180852094. 1, 6
- [23] Sodani, A. e G. S.Sohi: *Dynamic instruction reuse*. Proc. Int. Symp. Computer Architecture, páginas 194–205, 1998. 2, 10, 11

- [24] Steen, J. Van der, J.L. Coenders, S. Pasterkamp, A. Rolvink e J. Van Steekelenburg: *Computational reuse optimisation for stadium design*. Proceedings of the International Association for Shell and Spatial Structures, 2015. 2, 10
- [25] Stoer, M. e F. Wagner: *A simple min-cut algorithm*. J. ACM, 44(4):585—591, 1997. 19, 21
- [26] Teodoro, G., T. Pan, T. Kurc, J. Kong, L. Cooper, S. Klasky e J. Saltz: *Region templates: Data representation and management for high-throughput image analysis*. Parallel Computing, 40(10):589–610, 2014. x, 2, 7, 8, 9
- [27] Teodoro, George, Tahsin M. Kurc, Luís F. R. Taveira, Alba C. M. A. Melo, Yi Gao, Jun Kong e Joel H. Saltz: *Algorithm sensitivity analysis and parameter tuning for tissue image segmentation pipelines*. Bioinformatics, 2017. x, 7, 14
- [28] Wang, Weidong, A. Raghunathan e N.K. Jha: *Profiling driven computation reuse: An embedded software synthesis technique for energy and performance optimization*. Proceedings. 17th International Conference on VLSI Design, 2004. 2, 10, 11, 12
- [29] Weirs, V. G., J. R. Kamm, L. P. Swiler, S. Tarantola, M. Ratto, B. M. Adams, W. J. Rider e M. S. Eldred: *Sensitivity analysis techniques applied to a system of hyperbolic conservation laws*. Reliability Engineering & System Safety, 107:157–170, 2012. 1, 7
- [30] Wolstencroft, Katherine, Robert Haines, Donal Fellows, Alan Williams, David Withers, Stuart Owen, Stian Soiland-Reyes, Ian Dunlop, Aleksandra Nenadic, Paul Fisher, Jiten Bhagat, Khalid Belhajjame, Finn Bacall, Alex Hardisty, Abraham Nieva de la Hidalga, Maria P. Balcazar Vargas, Shoaib Sufi e Carole Goble: *The Taverna workflow suite: designing and executing workflows of web services on the desktop, web or in the cloud*. Nucleic Acids Res, 2013. 17